TRIBHUVAN UNIVERSITY
INSTITUTE OF ENGINEERING
PULCHOWK CAMPUS

THESIS NO: PUL078MSGtE013

SPECIFIC SITE RESPONSE ANALYSIS ON THE DIFFERENT EARTHQUAKE MOTION IN KATHMANDU VALLEY

by

Saroj Prasad Adhikari

A THESIS
SUBMITTED TO THE DEPARTMENT OF CIVIL ENGINEERING
IN PARTIAL FULFILLMENT OF THE REQUIREMENTS FOR THE DEGREE OF
MASTERS OF SCIENCE IN GEOTECHNICAL ENGINEERING

DEPARTMENT OF CIVIL ENGINEERING
LALITPUR, NEPAL

DECEMBER, 2023

COPYRIGHT©

TRIBHUVAN UNIVERSITY
INSTITUTE OF ENGINEERING
PULCHOWK CAMPUS
DEPARTMENT OF CIVIL ENGINEERING

The undersigned certify that they have read and recommended to the Department of Civil Engineering for acceptance, a dissertation entitled "**SPECIFIC SITE RESPONSE ANALYSIS ON THE DIFFERENT EARTHQUAKE MOTION IN KATHMANDU VALLEY**", submitted by **Saroj Prasad Adhikari** in partial fulfillment of the requirement for the award of the degree of **Masters of Science in Geotechnical Engineering**.

_____

Dr. Ram Chandra Tiwari
Supervisor
Assistant Professor
Institute of Engineering, Pulchowk Campus

_____

Dr. Dhundi Raj Pathak
External Examiner
Geotechnical Engineer

_____

Dr. Santosh Kumar Yadav
Assistant Professor
Program Co-ordinator
M.Sc. in Geotechnical Engineering

December 26, 2023

ABSTRACT

Seismicity is a critical concern in Nepal, particularly in the Kathmandu Valley, a region characterized by complex geological and geotechnical conditions. A Study presents a comprehensive site-specific response analysis of the Kathmandu Valley, employing the DEEPSOIL software for non-linear one-dimensional analysis to provide a thorough understanding of the valley's seismic behaviour, with a focus on the impact of five distinct earthquake motions, including the Gorkha Earthquake, Loma Gilroy Earthquake, Aftershocks of Gorkha Earthquake, Chi-Chi Earthquake, and Kobe Earthquake. The study offers a thorough summary of the amplification factors (AF) and earthquake events for seismic hazard assessments and engineering designs on how the ground motion is amplified or attenuated during seismic events. In comparison to other input motions, the result demonstrates a larger value of amplification factor for the Gorkha Earthquake motion and its aftershocks motion. The Kobe earthquake motion represents the remarkable exception, where amplification considerably decreased. Balaju stands out as the region with the highest ground motion amplification, which can be related to the existence of layers of gray loose micaceous silty fine sand in its subsurface geology. Additionally, this study compares its findings of the site-specific spectral acceleration with the recommended design spectra of IS 1893:2016 and NBC 205:2020 for a 5% damping ratio. Specifically considering the soft soil and very soft soil conditions as per IS 1893:2016 and NBC 205:2020, respectively, this analysis offers a critical evaluation of how the predicted spectral accelerations correspond with designated seismic design principles.

Keywords: Amplification, DEEPSOIL, PGA, PSA, Site Response

ACKNOWLEDGEMENT

TABLE OF CONTENTS

LIST OF FIGURES

LIST OF TABLES

LIST OF EQUATIONS

LIST OF ABBREVIATIONS

γ	Unit Weight
1D	One Dimensional
BH	Borehole
USGS	United States Geological Survey
V_s	Shear Wave Velocity
M_w	Moment Magnitude
M_l	Local Magnitude
M_b	Body-wave Magnitude
PGA	Peak Ground Acceleration
PHA	Peak Horizontal Acceleration
PSA	Peak Spectral Acceleration
S_a	Spectral Acceleration
AF	Amplification Factor
SPT	Standard Penetration Test
USCS	Unified Soil Classification System
DMG	Department of Mines and Geology
NBC	NEPAL NATIONAL BUILDING CODE
IS	Indian Standard

CHAPTER ONE: INTRODUCTION

1.1 Background

Kathmandu, the capital city of Nepal, is situated amidst the landscapes of the Himalayas and holds significant geological and seismic importance. It is located in an area of seismic activity due to the collision of the Indian and Eurasian tectonic plates, as shown in figure 1.1. Kathmandu faces the risk of earthquakes with varying intensities that can potentially cause severe damage to its infrastructure, historical monuments, and economy.

Figure 1.1: Collision of Indian and Eurasian Plates[1].

Nepal has a history of experiencing major earthquakes every 80–100 years, measuring above 7 on the moment magnitude (M_w) scale [2]. The Nepal-Bihar earthquake in 1934 (magnitude 8.3), the Udayapur earthquake in 1988 (magnitude 6.5), and more recently the Gorkha earthquake in 2015 ($M_w = 7.8$), have caused severe structural damage in Kathmandu and the surrounding area [3]. One such recent tragic occurrence (called Gorkha Earthquake 2015) struck on April 25, 2015, with a moment magnitude (M_w) of 7.8 and its epicentre 80 kilometers northwest of Kathmandu. The study of site-specific hazard analysis has been regarded as crucial since the

Kathmandu Valley is home to several architectural marvels and is densely populated, with a population of over 3.1 million (as of the census of 2021).

The 1934 Bihar-Nepal earthquake, with a magnitude of M 8.4 Richter Scale, indicated damage intensity ranging from IX to X on the Modified Mercalli intensity (MMI) Scale, had a devastating impact on the Kathmandu Valley[4]. The earthquake produced strong shaking in the valley, leading to widespread destruction of buildings and infrastructure. The strong ground shaking caused extensive damage, destroying a significant portion of the valley's building structure and causing significant loss of life and widespread destruction. The political, economic, and cultural center of the nation, the Kathmandu Valley, was shaken violently by the 1934 Bihar-Nepal earthquake, which also caused 40% of the valley's building stock to be damaged or destroyed([2]. Due to the turbulent past of the event, detailed economic damage and casualty statistics for this particular earthquake could not be easily accessible.

1.2   Problem Statement

The complex geological and geotechnical conditions of Kathmandu are seismically vulnerable, necessitating a thorough understanding of site-specific action. For analyzing ground responses across various geological settings, reliable calculation of amplification factors and fundamental time periods is essential. The value of the amplification factor changes depending on the input motion. In the study conducted by (Paudyal et al., 2012)[5], the spatial distribution of the dominant period of amplification was analyzed using a horizontal-to-vertical spectral ratio technique in Kathmandu Valley using microtremor measurement. In the context of seismic site response analysis, an amplification factor is the ratio of the input ground motion or reaction at the base of a site to the maximum ground motion or response at a certain point. It measures the extent to which ground motion is amplified or attenuated when it moves through various soil or geological conditions. In contrast, amplification factors are established based on the ratio of input ground motion to the calculated output motion through different analyses. The value of the amplification factor changes depending on the frequency content of seismic waves, seismic input characteristics, method of analysis, and so on.

The Kathmandu Valley experiences a range of earthquake magnitudes, contributing to diverse seismic hazards. Damages from prior earthquakes were more severe in Kathmandu Valley than in the rest of the country, despite the epicentre being located

several kilometres from the valley. Rapid urbanization as well as substantial residential building construction in the Kathmandu Valley demand the urgent need for seismic site response analyses, especially for shallow depths, to ensure the safety and resilience of the structures. Despite this variability, a comprehensive understanding of the amplification factors corresponding to different earthquake magnitudes has yet to be fully explored. Furthermore, the design spectrum provided by recent seismic design codes, such as the National Building Code (NBC) and the Indian Standard (IS), must be compared to the seismic response characteristics for specific sites with soft soil sediments.

1.3   Objective

The objectives of this study are:

- To analyze the amplification factors (PGAoutput/PGAinput) based on the characteristics of the different input ground motions.

- To determine how geotechnical as well as geological factors influence different seismic activity at shallow depths in Kathmandu Valley.

- To compare the spectral acceleration of the site against the seismic standard NBC 105:2020 and IS 1893:2016

- To analyze the seismic site response results regarding the devastation brought on by the 2015 Gorkha earthquake and its aftershocks

1.4   Location of Study Area

Historically, Kathmandu Valley used to be believed to be a lake that dried up in the Late Pleistocene [6, 7]. It is considered to be filled with fluvial and lacustrine deposits of more than 550m thickness from the late Pliocene to Pleistocene age [8] bounded to the south by the Main Boundary Thrust (MBT) and to the north by the main central thrust (MCT), as shown in figure 1.2.

The typical lacustrine deposits found in the Kathmandu Valley have drawn several geoscientists from around the globe[10].

3
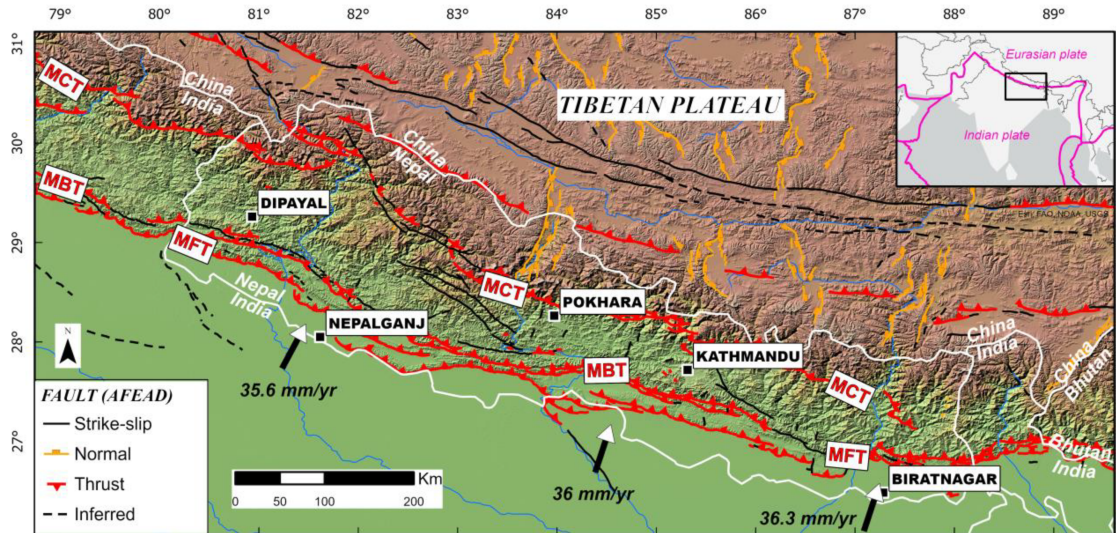
Figure 1.2: Structural map of Nepal and Himalayan mountains showing the major thrusts [9]

Figure 1.3 illustrates the Kathmandu Valley's geological background with various formations. From the chronological sequence, the older sediments start in the Lukundol formation, which is covered by the Chapagon, Boregaon and Pyangaon formations. The much younger formations are the Gokarna, Thimi and Patan formations, followed by the Kalimati formations. The northern part of the valley mainly comprises poorly sorted sediments and loose, unconsolidated coarse sands, silts, and gravel. The southern region is composed of highly plastic clay and silt, with coarse sediments above and below the deposits at certain places. The central part comprises three formations: Bagmati, Kalimati and Patan formation. The Bagmati Formation constitutes the lower part of the central basin with coarse sands, gravels, and boulders, while the Kalimati Formation consists of dark grey carbonaceous beds of lacustrine deposits interbedded with medium- to coarse-grained sands and the Patan Formation with medium- to coarse-grained sand.

1.5   Limitations of the Study

- The study is carried out in a single dimension, which simplifies the model and may not capture all complexities. A 2D or 3D analysis could provide a more complete picture of the site reaction.

- Soil layers are modelled only up to shallow depths (i.e., 8 to 20 m), due to the lack of availability of data, whereas considering site response up to the bedrock would provide a more realistic assessment of seismic behaviour.
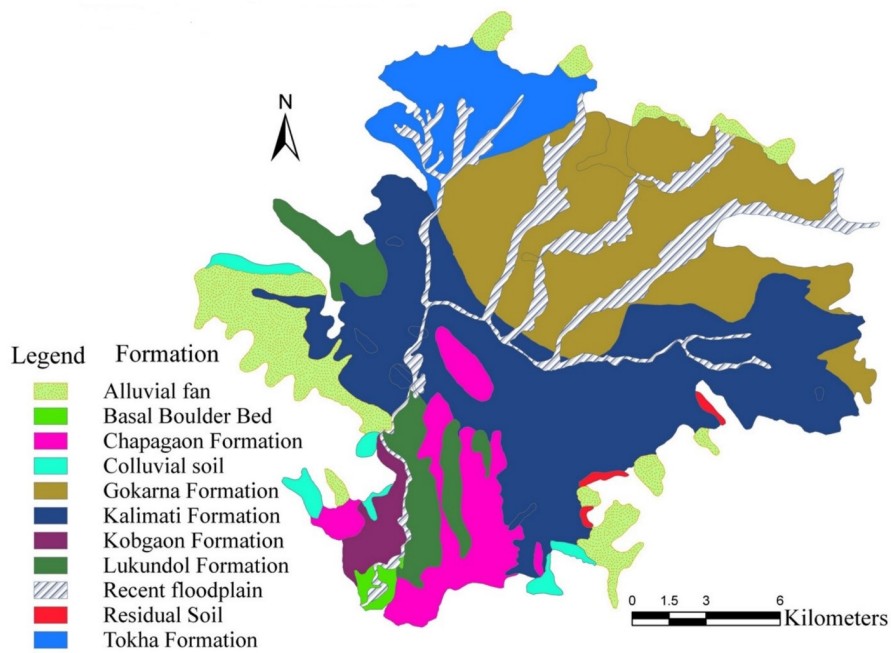
Figure 1.3: Regional Geological Map of Kathmandu Valley (DMG)

- Statistical and dynamic geotechnical parameters such as shear modulus, dynamic shear modulus, damping ratio, shear wave velocity(V_s), and unit weight(γ) are often derived from standard empirical correlations rather than precise laboratory data.

- The study is performed on a total stress analysis, which may not fully account for the pore water pressure generation and effective stress changes along the depths during an earthquake.

CHAPTER TWO: LITERATURE REVIEW

2.1 Seismicity of Nepal

Nepal is located in one of the world's most active continental collision zones (i.e., in between the Eurasian plate and Indian plate, as shown in figure 1.1, the Himalayas, where the probability of earthquake occurrence is very high. So, the entire nation of Nepal is seismically active. Over history, the region has persistently faced the impact of repeated seismic events that have significantly shaped its landscape and impacted local communities. According to historical records, the Kathmandu Valley has witnessed numerous significant earthquakes throughout its history. Major historical earthquake damage in Nepal was reported in 1255, 1408, 1681, 1803, 1810, 1833, and 1866 [11] and recent events include 1934, 1988, 2015, and 2023, all of which ruined a great number of lives, residences, and economics.

A moment-magnitude (M_w) 7.8 earthquake struck Gorkha on April 25, 2015, and was followed by a series of severe aftershocks, including a magnitude 7.3 earthquake on May 12, 2015. The epicenter (N: 28.1470°; E: 84.7080°) of the main shock was located about 77 km northwest of Kathmandu at a focal depth of approximately 15 km (USGS, 2015). The earthquake caused a heavy toll of about 9,000 dead, more than 23,000 injured, and more than U.S. \$5.0 billion in losses[12]. Recently, the western part of Nepal has experienced significant seismic activity. On October 3, 2023, a 6.3 local magnitude(M_l) earthquake struck Bajhang (DMG), destroying 334 houses and partial damage to 1,185 others (source: ECHO, as published on October 5, 2023). Similarly, on November 3, 2023, Jajarkot was hit by a 6.4 local magnitude earthquake(M_l) (DMG), tragically claiming the lives of 157 individuals and injuring 349 others (source: ADRA Nepal, as published on November 7, 2023). Recent reports indicate substantial destruction, with at least 4,000 houses being either completely or partially destroyed. In addition to the primary earthquakes, the western part of Nepal continues to experience aftershocks, underscoring the persistent seismic activity in the region.

2.2 Local Site Effects

The behaviour of the ground during an earthquake can affect the impact of seismic occurrences on structures and communities. This phenomenon is known as site response. It's how the local geology and soil properties affect the way seismic waves propagate and interact with the ground, as shown in figure 2.1. The significance of
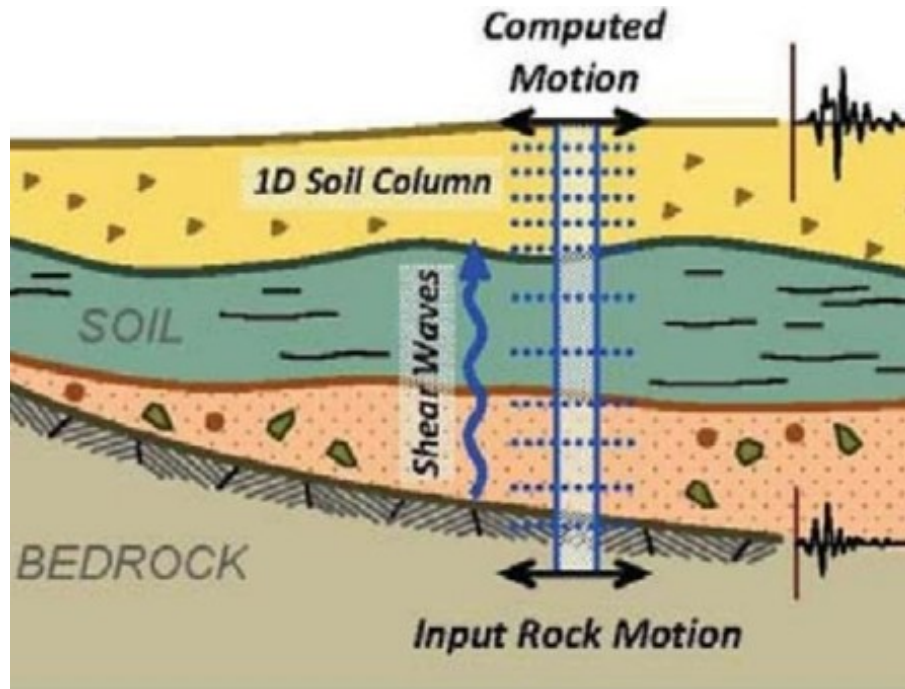
Figure 2.1: Graphical description of 1-D site response analysis[13]

local site effects became evident following the Michoacán earthquake of 1985, with its epicenter located in Michoacán, approximately 320 km from Mexico City. Despite causing only moderate damage near its epicenter, located near the Pacific coast of Mexico, the earthquake resulted in extensive damage some 350 km away in Mexico City. Similar patterns have been observed in subsequent earthquakes, including the Northridge earthquake (1994), the Kobe earthquake (1995), the Bhuj earthquake (2001), the Kashmir earthquake (2005), the Sichuan earthquake (2008), the Chile earthquake (1985), and the Haiti earthquake (2010), illustrating the significant role of local site conditions on earthquake damage[14, 15, 16, 12]. Notably, the 1999 Chi-Chi earthquake in Taiwan and the 1989 Loma Prieta earthquake in California serve as significant examples of local site effects[17, 18].

A major problem in the Kathmandu Valley has been consistently proven by several studies: because of the peculiar subsurface structure of the valley, there is an amplification of ground motion and consequently higher sensitivity to earthquake damage [19, 20, 21, 5]. Strong site effects have been identified in the valley, according to (Dixit et al., 2000) [2], (Hough & Bilham, 2008) [19] and (Mugnier et al., 2011)[21], based on evidence of damage severity in the valley from previous earthquakes, notably the 1934 Bihar-Nepal earthquake[12].

2.3 Previous research on-site response analysis

The amplification effect of local soil in various parts of the Kathmandu Valley was examined in previous studies of (Dixit et al., 2000[2]; Gaha et al., 2022[3]; Maskey & Datta, 2004[4]; Paudyal et al., 2012[5];Pandey, 2000;[22]). These studies have primarily focused on the impact of unconsolidated soil sediment deposition on the amplification of seismic waves. The collective findings suggest that the soil amplification effect exhibits variations across different locations within the Kathmandu Valley. The presence of unconsolidated soil sediment, known to enhance the amplification of seismic waves during earthquakes, explains this spatial variability.

(Gaha et al., 2022)[3] conducted 1D equivalent linear ground response analysis in Kathmandu Valley with three different earthquake motions and showed that the amplification was higher for the Gorkha earthquake compared to other input motions. (Kawan et al., 2022)[23] conducted site-specific ground response analysis using both equivalent linear and non-linear analysis methods and developed the seismic hazard maps in terms of the peak ground acceleration, amplification factor, peak spectral acceleration, and pre-dominant periods of the Bhaktapur city.

(Kumar et al., 2020)[24] performed non-linear ground response analysis and liquefaction potential assessment considering 10 borehole log locations at Kathmandu and concluded that Jamal, Chyasal and Khulamanch were identified as being at the highest risk. The input ground motion for this study was of Gorkha earthquake motion recorded at five different locations within the Kathmandu valley.

(Gautam et al., 2017)[25] concluded that the nonlinear one-dimensional seismic site response analysis of soft soil deposits in Kathmandu Valley reveals that the peak ground acceleration varies between 0.10 to 0.50 g, indicating de-amplification during strong earthquakes.

(Sharma et al., 2017)[12] concluded that the damage patterns observed during the Gorkha earthquake in Nepal were influenced by various factors such as local site conditions, topography, and basin edge effects. The presence of soft alluvial soil deposits in the Kathmandu Valley also contributed to the amplification of ground shaking.

(A. Kumar et al., 2017)[26] observed a low value of amplification factor for high peak horizontal acceleration in central, western, and southern parts of Nepal, indicating nonlinear soil behavior. (Puri et al., 2018)[27] conducted the equivalent

linear earthquake response analysis using three earthquake time history motions (Chamoli Earthquake, Sikkim Earthquake, and Uttarkashi Earthquake) in Haryana using DEEPSOIL.

2.4 Uniqueness of Research

The uniqueness of this thesis stems from its distinctive approach to synthesizing and extending the insights derived from prior studies on the amplification effect of local soil in the Kathmandu Valley. While existing literature has predominantly focused on the role of unconsolidated soil sediment in influencing seismic wave amplification, this thesis uniquely builds upon these foundations by systematically examining and comparing ground responses across five different earthquakes.

Prior studies, such as those by (A. Kumar et al., 2017)[26] and (Sharma et al., 2017)[12], have touched upon the nonlinear behaviour of soil and its impact on amplification factors, but none have undertaken a comprehensive analysis incorporating multiple seismic events as undertaken in this research. The inclusion of earthquakes with varying magnitudes, such as the Gorkha earthquake 2015 and its aftershocks, the Kobe earthquake 1995, the Loma Prieta earthquake 1989, and the Chi-Chi earthquake 1999, adds a novel dimension to the understanding of the local site effect in the Kathmandu Valley. This thesis facilitates a distinctive contribution to the field of geotechnical earthquake engineering by exploring the complex dynamics of various soil types and how they react to a range of seismic events. These insights are extremely helpful in improving seismic risk assessments and engineering plans that are customized to the region's particular seismic characteristics.

CHAPTER THREE: METHODOLOGY

3.1   Introduction

This chapter deals with the methodology followed to carry out the present study. The methodologies of research are presented in the flowchart, as shown in figure 3.1
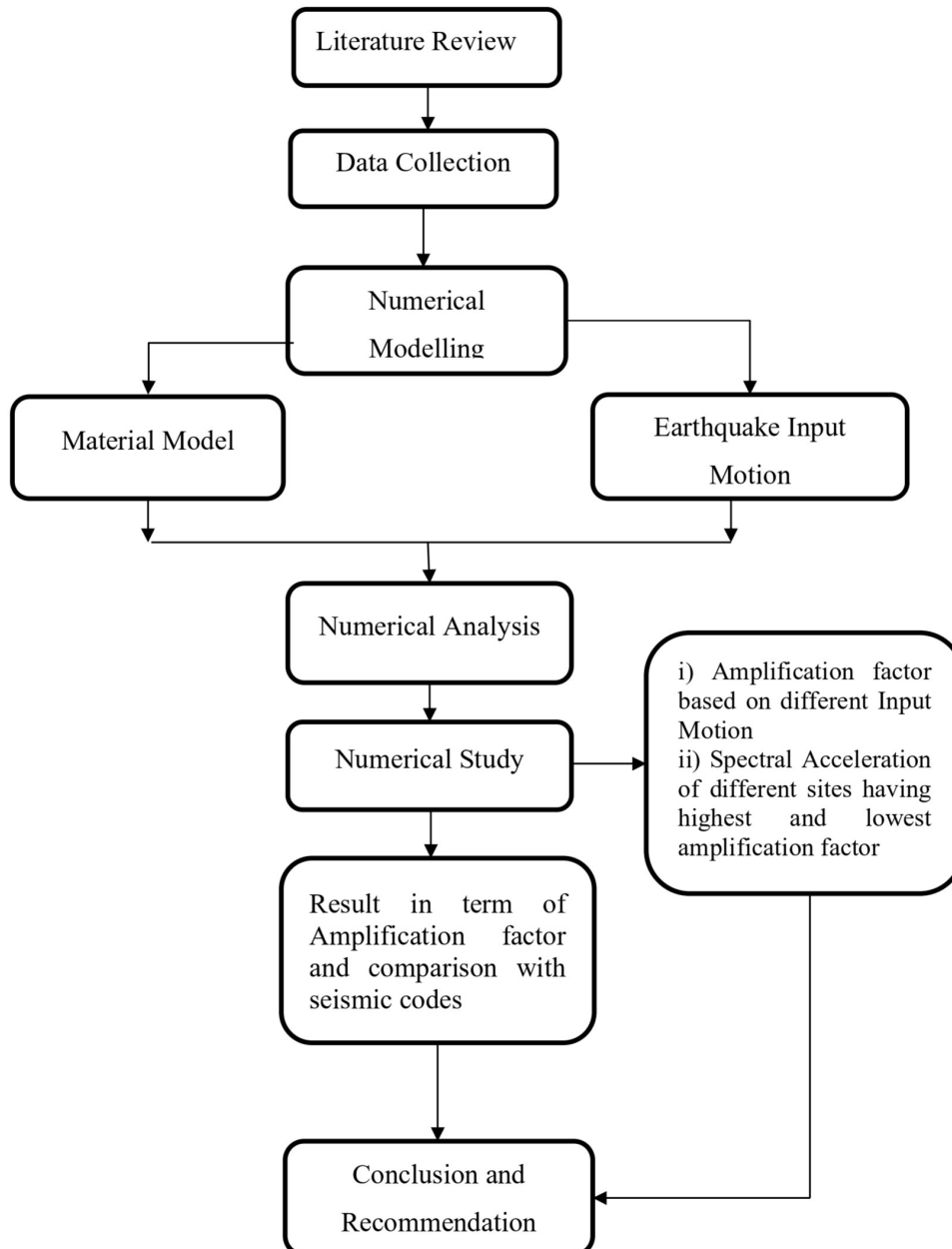
Figure 3.1: Flow Chart of Methodology

3.2 Data Collection

The SPTs conducted at different locations in Kathmandu Valley were obtained from site investigation reports and through journals, engineering consultancies, and Kathmandu Upatyaka Khanepani Limited (KUKL). The borehole logs included visual classification of soil (by USCS) and records of SPT values at every depth interval of 1.5 m. At each depth where the SPT test was carried out, the number of blows was recorded at every penetration depth interval of 150 mm until a total depth of penetration of 450 mm was reached. The number of blows recorded for the first 150mm is not taken into consideration (also called seating penetration). The number of blows recorded for the last two 150mm intervals is added to give the standard penetration number (N).

For the study, borehole log data from 33 different locations drilled at depths of 8 to 30m were assessed. The spatial distribution of the borehole log is illustrated in figure 3.2.
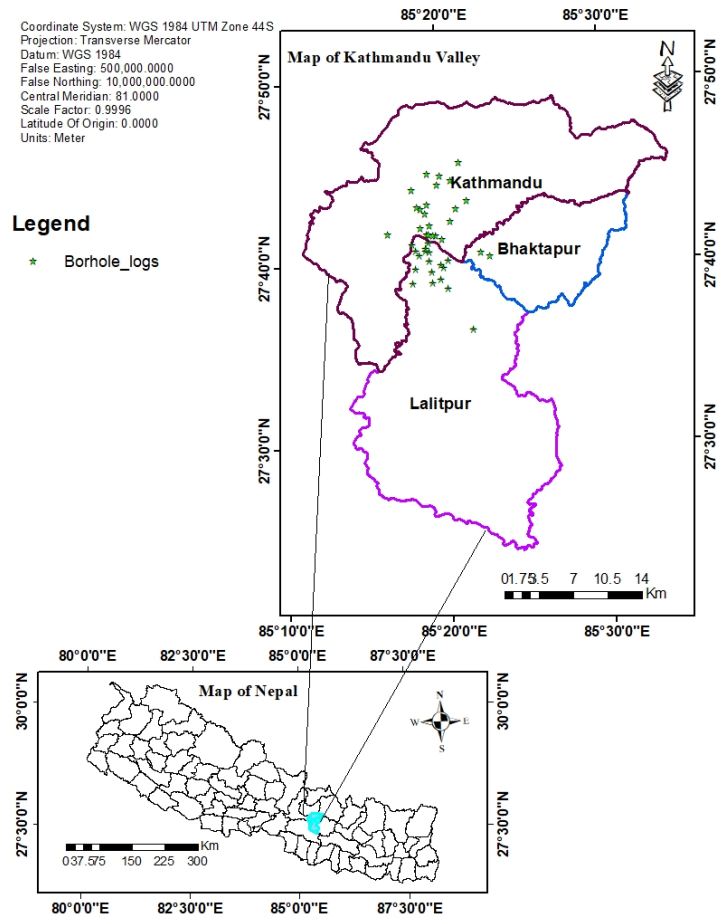
Figure 3.2: Study area map and borehole log location

11

3.3 DEEPSOIL

The features of DEEPSOIL, a specialist software program made for simulating ground motion amplification in layered soil profiles, are utilized in this thesis' seismic site response study. DEEPSOIL is a unified 1D equivalent linear, equivalent linear and nonlinear site response analysis platform. DEEPSOIL excels in providing high-fidelity simulations of seismic site response, capturing the complex interplay between seismic waves and diverse geological conditions. In this study, DEEPSOIL was employed to model the ground response to five distinct earthquake motions in the different locations of Kathmandu Valley, offering a minute exploration of how varying magnitudes and frequencies impact soil-structure interaction. The methodology section delves into the specifics of the DEEPSOIL application, detailing the input parameters, simulation settings, and any validation procedures undertaken to ensure the accuracy of the results. The choice of DEEPSOIL is motivated by its unique features, including its ability to handle nonlinear soil behaviour, making it a suitable and robust tool for this comprehensive analysis. This dedicated section elucidates the pivotal role of DEEPSOIL in advancing the understanding of ground response in the context of seismic hazard assessment in the Kathmandu Valley.

The choice of DEEPSOIL software for this research is rooted in several compelling reasons. DEEPSOIL, a specialized tool in Geotechnical earthquake engineering, was selected due to its advanced capabilities in simulating ground motion amplification in layered soil profiles, such as:

- User-Defined Input Parameters: Users can input various parameters, including soil layer properties (thickness of each soil layer, material properties of each layer like shear wave velocity, density, damping characteristics, Poisson's ratio, Young's modulus), site configuration (water table depth, ground surface elevation), ground motion input (earthquake records/acceleration time histories for input motions, the frequency content of the seismic waves), analysis setting (analysis type like linear, equivalent linear, or nonlinear), damping ratios, numerical parameters for the analysis algorithm, and boundary conditions (applied stresses or displacements at the base of the soil profile).

- Dynamic Soil Consideration: DEEPSOIL dynamically models the evolution of soil properties under different levels of ground shaking and damping characteristics of the soil layers, analyzes the changes in strain and stress within the soil

layers as seismic waves pass through, and incorporates nonlinear behaviour in the soil layers that can arise due to large ground motions.

- Comprehensive Output Results: DEEPSOIL provides a comprehensive set of output results that are crucial for understanding the seismic site response and assessing the impact of ground shaking on soil layers. The specific output results may vary based on the analysis settings and user-defined parameters, but common outputs include amplification factors, phase differences, time histories of ground motion, response spectra, deformation profiles, displacement and velocity profiles at different depths within the soil profile, and stress and strain profiles within the soil layers.

- Model Validation: DEEPSOIL predictions can be rigorously validated through comparisons with accurate real-world measurements or by bench-marking against other analytical methods. This validation process ensures the precision and reliability of the simulation results, contributing to the accuracy of the seismic analysis.

3.4 Material Model

3.4.1 Unit Weight

Due to the absence of the Unit Weight(γ) of soil at each layer of the borehole log from the lab test, the Unit weight of soil strata is correlated with Average soil engineering properties according to USCS classification as per (Krahenbuhl & Wagner, 1983)[28] as shown in Table 3.1

3.4.2 Shearwave Velocity(V_s)

Shear wave velocity (V_s) is a measure of the speed at which shear waves propagate through a material. Shear waves are a type of seismic wave that cause particles in a material to move perpendicular to the direction of wave propagation, as opposed to compression waves (P-waves) which cause particles to move parallel to the direction of wave propagation. Shear wave Velocity(V_s) is an important property in seismology and geotechnical engineering, as it is used to estimate the stiffness and strength of soil and rock formations. The measurement of V_s is typically done through seismic surveys, where shear waves are induced in the ground and the time it takes for the waves to travel through the material is measured. In the absence of geophysical experiments, the shear wave velocity was approximated by correlating with SPT-N

Table 3.1: Average soil engineering properties according to USCS classification[28]

Group	Classification	Unit weight(γ) (kN/ m3)		Friction angle (degrees)		Cohesion (kN/ m2)	
GW	(Clean gravel, well-graded)	20	±2.50	40	±5	0	
GP	(Clean gravel, poorly graded)	19	±3.00	38	±6	0	
GM	(Silty gravel, poorly graded)	21	±2.50	36	±4	0	
GC	(Clayey gravel, little fines)	20.5	±2.00	34	±4	0	
GM-ML	(Silty gravel many fines)	21.5	±2.50	35	±5	0	
GM-GC	(Silty to clayey gravel)	21.9	±2.00	33	±3	2	±2
GC-CL	(Clayey gravel many fines)	21	±2.00	29	±4	3	±3
GC-CH	(Clayey gravel, fines with high plasticity)	19.5	±2.00	28	±4	4	±4
SW	(Clean sand, well graded)	19.6	±2.00	38	±5	0	
SP	(Clean sand, poorly graded)	18.5	±2.50	36	±6	0	
SM	(Silty sand little fines)	20	±2.50	34	±3	0	
SC	(Clayey sand, little fines)	19.6	±2.00	32	±4	0	
SM-ML	(Silty sand many fines)	20	±2.00	34	±3	0	
SM-SC	(Silty to clayey sand)	21	±2.00	31	±3	5	±5
SC-CL	(Clayey sand many fines)	20.5	±2.00	28	±4	5	±5
SC-CH	(Clayey sand fines with high plasticity)	18.5	±2.00	27	±3	10	±10
ML	(Silt)	19	±2.50	33	±4	0	
CL-ML	(Silt to clayey silt)	21	±1.50	30	±4	15	±10
CL	(Clayey silt)	20	±1.50	27	±4	20	±10
CH	(Clay)	17.5	±1.50	22	±4	25	±10
OL	(Organic clayey silt)	12	±1.50	25	±4	10	±5
OH	(Organic clay)	15.6	±1.50	22	±4	10	±5
MH	(Inorganic silt of high compressible)	15.6	±1.50	24	±6	5	±5

values. Several empirical correlations relate the shear wave velocity (V_s) of soils to the SPT-N value.

The Kathmandu basin is made up of a thick succession of fluvial and lacustrine sediments from the Plio-Pleistocene to the Holocene epoch. These deposits are primarily composed of unconsolidated to semiconsolidated sand, gravel, peat, silt, clay, and carbonaceous black clay, known locally as "Kalimati." These sediments exist unevenly on top of Paleozoic rocks from the Phulchauki Group and partially from the Bhimphedi Group of the Kathmandu Complex, which makes up the Mahabharat Range that surrounds the Kathmandu Valley[7]. In the valley basin, the sediment thickness ranges from 550 to 600 m (DMG, 1998) or exceeds 650 m in the center region [29, 30, 31].

(Ohta & Goto, 1978)[32] proposed the shear wave velocity based on geology (i.e., based on deposition & age) and uncorrected SPT for all soils,i.e.,

$$Vs = 134.2N^{0.27} \tag{3.1}$$

The shear wave velocity values obtained from equation 3.1 in comparison to the shear wave velocity values proposed by JICA (2001) are examined. The outcomes of this comparison exhibit a remarkable level of concurrence, with the values falling consistently within the range of 150 to 350 m/s. This alignment between the shear wave velocity figures obtained from the different sources suggests a harmonious agreement and lends confidence to the accuracy and reliability of the data. (Kawan et al., 2022)[23] also employed equation 3.1 to compute shear wave velocities and subsequently averaged them using a relationship based on depth, similar to the approach proposed by (Ohta & Goto, 1978)[32]. Moreover, equation 3.1 has a correlation coefficient of 0.784 and a probable error of 24.2%, so it can provide a reliable estimate of shear wave velocity of soil profile having SPT value. The Plot of shear-wave velocity across depth using 3.1 for different locations is illustrated in APPENDIX B.

3.4.3 Pressure-Dependent Modified Kodner Zelasko (MKZ) Soil Model

Using the DEEPSOIL, one-dimensional non-linear ground response assessments have been performed. The cyclic behaviour of soil is represented by the non-linear time

domain analysis. To accurately model ground response using the nonlinear methodology in the time domain, the equation of motion needs to be solved for each small-time increment:

$$M\ddot{u} + C\dot{u} + Ku = F(t) \tag{3.2}$$

where M is the mass matrix, C is the damping matrix, K is the stiffness matrix., u is the displacement vector, ü is the acceleration vector, u is the velocity vector, and F(t) is the force vector applied at each time increment[33].

The initial backbone curve for the first loading cycle is described by the hyperbolic stress-strain model, which was initially developed by (R. L. Kondner, 1963)[34] and then revised by (Matasović & Vucetic, 1993)[35]and (Hashash et al., 2010)[36]. Modelling the soil stiffness degradation with the developing pore water pressure as the parameter results in the stress-strain behaviour in the succeeding cycles. The DEEPSOIL 7.0 algorithm uses the curve fitting approach created by (Hashash et al., 2010)[37], commonly known as MRDF-UIUC, to perform non-linear non-Masing analysis. This procedure altered the (G. Masing, 1926)[38]and extended Masing rules. To produce the stress-strain curves, the loading and unloading/reloading conditions are represented by equations 3.3 and 3.4, respectively.

$$\tau = \frac{G_0\gamma}{1 + \beta\left(\frac{\gamma}{\gamma_r}\right)^s} \tag{3.3}$$

$$\tau = F(\gamma_m)\left[2\frac{G_0\left(\frac{\gamma-\gamma_{\text{rev}}}{2}\right)}{1 + \beta\left(\frac{\frac{\gamma-\gamma_{\text{rev}}}{2}}{\gamma_r}\right)^s} - \frac{G_0(\gamma-\gamma_{\text{rev}})}{1 + \beta\left(\frac{\gamma_m-\gamma_r}{2}\right)^s}\right] + \frac{G_0(\gamma-\gamma_{\text{rev}})}{1 + \beta\left(\frac{\gamma_m-\gamma_r}{2}\right)^s} + \tau_{\text{rev}} \tag{3.4}$$

where G_0 represents the Initial shear modulus, τ denotes Shear strength, γ is the given shear strain, γ_r corresponds Reference shear strain, γ_{rev} signifies the reversal shear strain, τ_{rev} represents the reversal shear stress, γ_m stands for the maximum shear strain, $F(\gamma_m)$ represents a reduction factor, β and s are the Model parameters.

3.4.4 Modulus Reduction and Damping curves

Modulus reduction curves and damping ratio curves have been selected based on different soil properties. In the absence of site-specific modulus reduction and damping curves, standard curves proposed by [39] and [40] for clay and sand are used respectively. A plot of the modulus reduction and damping curve adopted in the study in this study is shown in Figure 3.3 and 3.4.
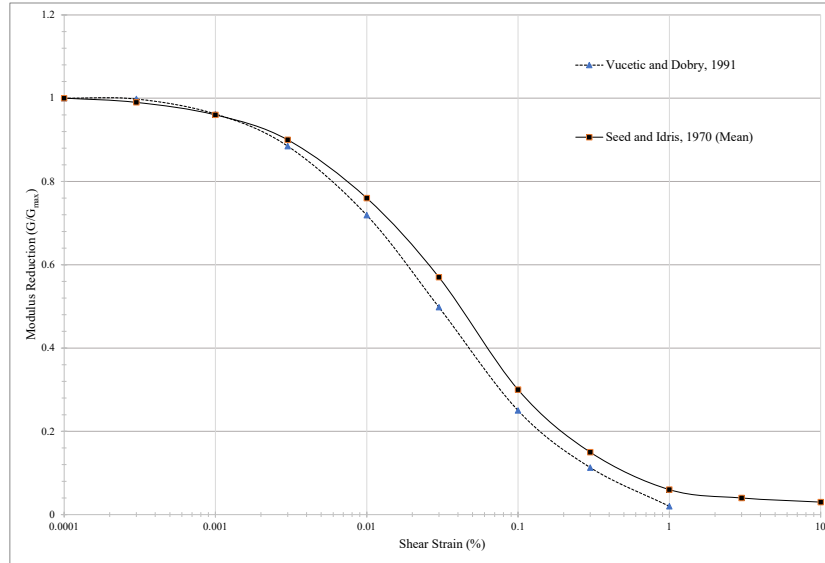
Figure 3.3: Dynamic property of soil, modulus Reduction curve[39] [40]

3.5 Input Motion

The ground response study involves producing or obtaining an acceleration time history that corresponds to the highest dynamic loading estimated at the site of interest. Different input ground motions refer to variations in the characteristics and properties of seismic waves that affect the Earth's surface during an earthquake. Seismic waves can vary in amplitude, frequency content, and duration, among other factors. These variations can be due to differences in the earthquake source, geological conditions, and the path the waves take as they propagate through the Earth. For this study, five earthquakes, the Gorkha Earthquake (2015), the Kobe Earthquake (1995), the Loma-Gilroy Earthquake(1989), the Chi-Chi Earthquake (1999) and the Aftershock of the Gorkha Earthquake (2015) are selected.
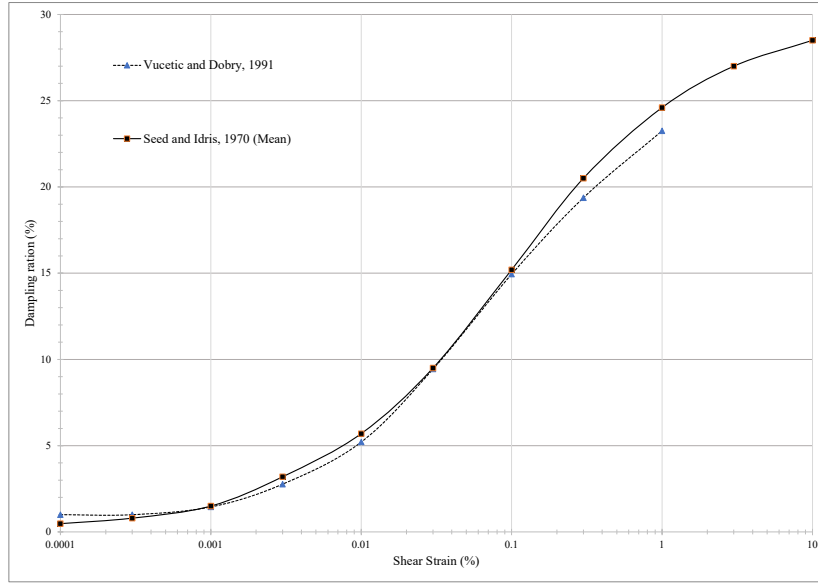
Figure 3.4: Dynamic property of soil,Damping Ratio curve[39] [40].

The selection of input motion includes a variety of seismic intensities measured at different stations, which are tabulated in table 3.2. With a PGA of 0.156 g (NS), the Gorkha earthquake serves as a benchmark for recent seismic activity in Nepal, and the aftershocks' lower PGA of 0.055g helps investigate residual ground shaking impacts. The Chi-Chi and Loma-Gilroy earthquakes, with PGAs of 0.18g and 0.17g, respectively, offer insights into regions with more moderate seismic danger. In contrast, the Kobe earthquake, with a high PGA of 0.8g, indicates severe seismic circumstances. Figure 3.5 displays PGA variations among five earthquake motion records, showcasing differing seismic intensities, from the lowest PGA of 0.055g in aftershocks to the highest PGA of 0.8g in the Kobe earthquake.

Table 3.2: Earthquake Time History Data

S. N	Time History	Date	Recording Station	Magnitude	Stations to Epicenter(km)	PGA(g)
1	Gorkha Earthquake	2015-04-25	Kritipur municipality	7.8 M_w	77 Km	0.156g
2	Chi-Chi	1999-09-21	Taichung, Taiwan	7.6 M_w	34.8 Km	0.18g
3	Kobe	1995-01-17	JMA station	6.9 M_w	0.6 Km	0.82g
4	Lima-Gilroy	1989-10-17	Gilroy Array Station 6	6.9 M_w	12.2 Km	0.17g
5	Aftershock of Gorkha Earthquake	2015-04-25	Kritipur municipality	5 M_b	7.14 Km	0.055g
Source: https://www.strongmotioncenter.org/						

18
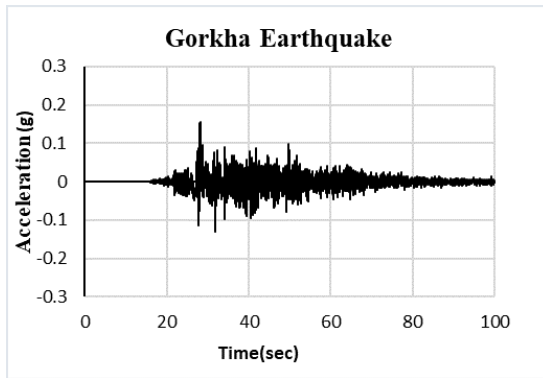
(a)
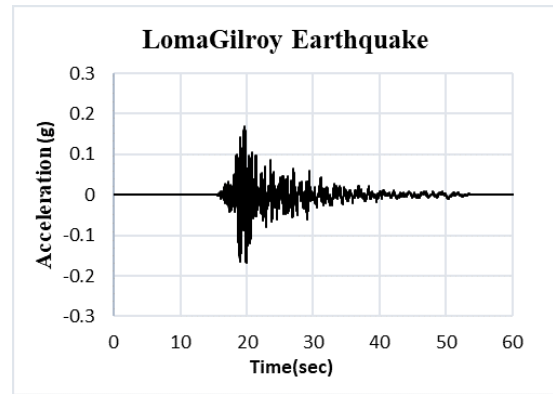
(b)
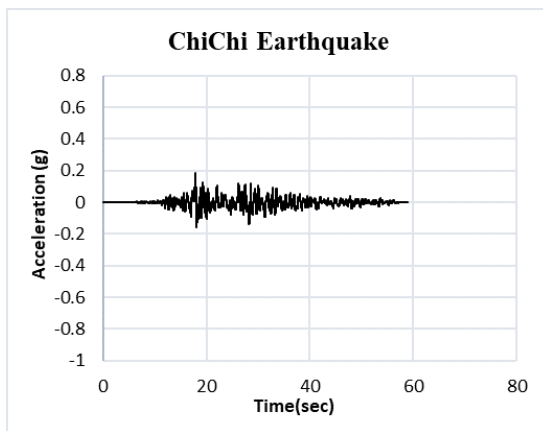
(c)
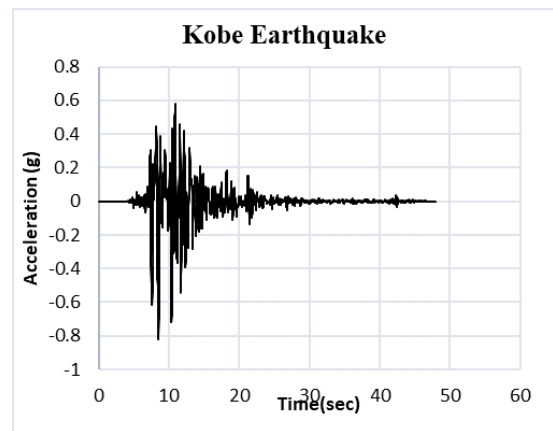
(d)
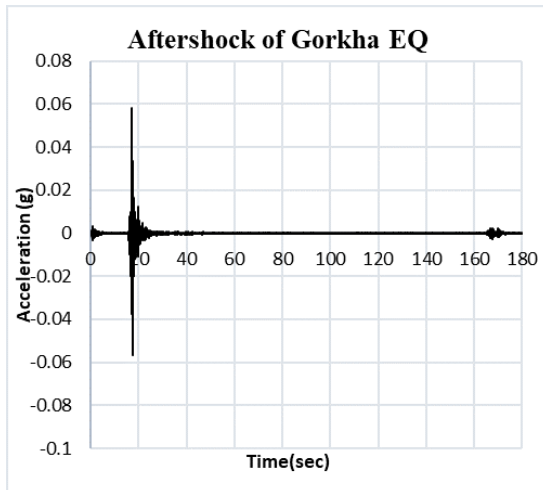
(e)

Figure 3.5: a,b,c,d,e: Variation in Peak Ground Acceleration (PGA) across five earthquake motion records, highlighting seismic intensity differences

CHAPTER FOUR: RESULTS AND DISCUSSION

4.1 Introduction

In this section, the exploration of the seismic site response analysis begins with the presentation of a concise table summarizing amplification factors (AF) observed at various sites within the Kathmandu Valley. Table 4.1 illustrates the dynamic behaviour of soil layers under different earthquake motions characterized by varying peak ground acceleration (PGA). This preliminary overview establishes the context for a thorough examination of AF patterns and their detailed interpretation in the subsequent sections. Table 4.1 provides a glimpse into the observed amplification factors at distinct locations within the study area, laying the foundation for a comprehensive seismic site response analysis. The borehole log data of distinct locations are attached in Appendix A.

From table 4.1, it is observed that site response is complicated, as seen by the wide variation in amplification factors across different areas and seismic events. The analysis of amplification ratios reveals a notable similarity between the Gorkha and Loma-Gilroy earthquakes. The amplification factor observed during the Chi-Chi earthquake was moderate. However, it's interesting to observe that higher amplification factors are associated with the aftershock of the Gorkha earthquake. In comparison, lower amplification factors tend to be observed during the Kobe earthquake, as shown in figure 4.1 and figure 4.2.

4.2 Variability of Amplification across Different Earthquake Motions

The amplification factors (AF) observed across the Kathmandu Valley exhibit notable variations in response to different seismic events, each characterized by distinct peak ground accelerations (PGA). In the case of the Gorkha earthquake, which had a PGA of 0.156g, the amplification factors across borehole locations ranged from 0.83 to 1.904. Moving to the aftershocks of the Gorkha earthquake, with a lower PGA of 0.055g, the corresponding amplification factors exhibited a different pattern, ranging from 0.958 to 2.260. This range indicates the diverse soil dynamics at play as well as how various study area sites responded to the particular characteristics of the Gorkha earthquake and its aftershocks.

Table 4.1: Amplification Factors at Various Sites during Different Earthquake Motion in Kathmandu Valley

| S.N	Borehole Log Notation	Location	AF based on different Input Motion				
			Gorkha	Chi-chi	After-shocks	Kobe	Lima Gilroy
1	BH-K1	Thapathali	1.212	1.898	1.184	0.423	1.35
2	BH-K2	Anamnagar	1.217	1.522	1.168	0.416	1.321
3	BH-K3	New Baneswor	1.395	1.813	1.336	0.397	1.211
4	BH-K4	Balaju	1.904	2.156	1.264	0.796	2.057
5	BH-K5	Maharajung	1.729	2.139	1.35	0.803	1.848
6	BH-K6	Gongabu	1.53	1.992	1.4	0.543	1.414
7	BH-K7	Budhanilkantha	1.814	2.085	1.242	0.907	1.958
8	BH-K8	Basbari	1.812	1.827	1.207	0.824	1.829
9	BH-K9	Basundhara	1.78	2.098	1.229	0.911	1.909
10	BH-K10	Boudha	1.711	2.158	1.382	0.858	1.738
11	BH-K11	Thamel	1.303	1.43	1.191	0.428	1.449
12	BH-K12	Babarmal	1.119	1.298	1.039	0.342	1.145
13	BH-K13	Sorahkhutte	1.753	2.26	1.415	0.701	1.896
14	BH-K14	Lazimpat	1.357	1.627	1.44	0.527	1.364
15	BH-K15	Durbaramarg	1.56	2.097	1.32	0.747	1.689
16	BH-K16	Battisputali	1.712	2.182	1.348	0.81	1.762
17	BH-K17	Putalisadak	0.905	1.103	0.833	0.25	0.976
18	BH-K18	Maitighar	1.112	1.375	1.169	0.379	1.201
19	BH-K19	Chabahil	1.782	1.956	1.208	0.934	1.913
20	BH-L1	Imadol	1.455	1.773	1.404	0.53	1.378
21	BH-L2	Pulchowk	1.506	1.813	1.281	0.766	1.48
22	BH-L3	Kupandol	1.125	1.409	1.03	0.353	1.196
23	BH-L4	Kumaripati	1.561	1.502	1.163	1.001	1.754
24	BH-L5	Balkumari	1.137	1.315	1.048	0.385	1.3
25	BH-L6	Sanepa	1.151	1.291	1.231	0.467	1.166
26	BH-L7	Hariharbhawan	0.832	0.958	0.681	0.205	0.77
27	BH-L8	Gwarko	0.998	1.184	0.946	0.333	1.09
28	BH-L9	Hatiban	1.323	1.711	1.311	0.462	1.331
29	BH-L10	Patan	1.52	2.089	1.301	0.509	1.405
31	BH-L12	Jawalkhel	1.451	1.744	1.371	0.542	1.319
32	BH-B1	Chardobato	1.211	1.666	1.201	0.427	1.273
33	BH-B2	Gattaghar	1.058	1.264	0.958	0.334	1.115
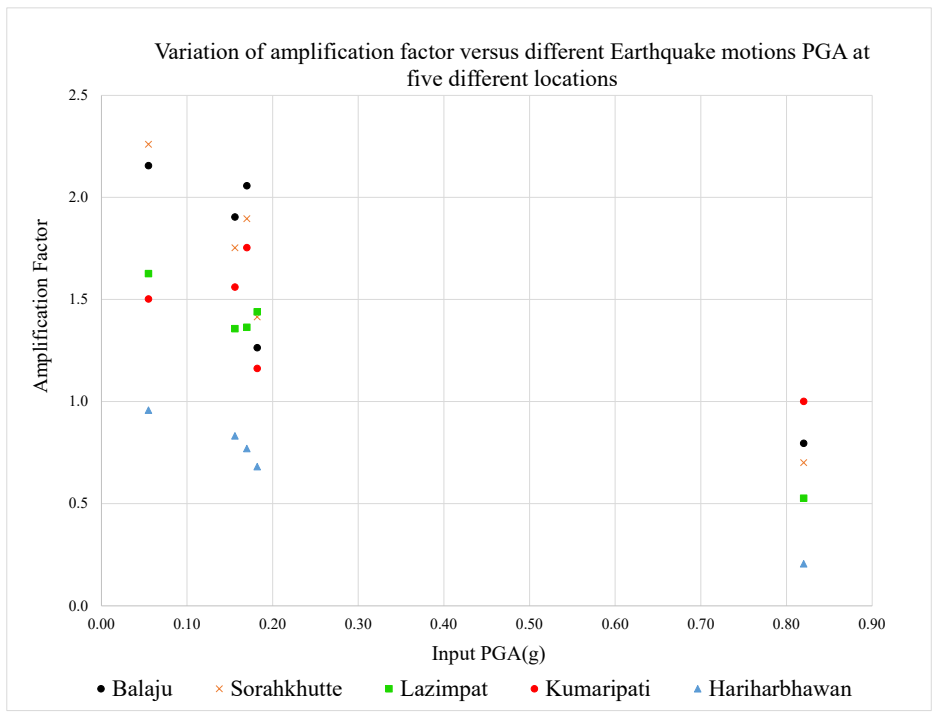
Figure 4.1: Variation of AF vs Input PGA for specific five Locations
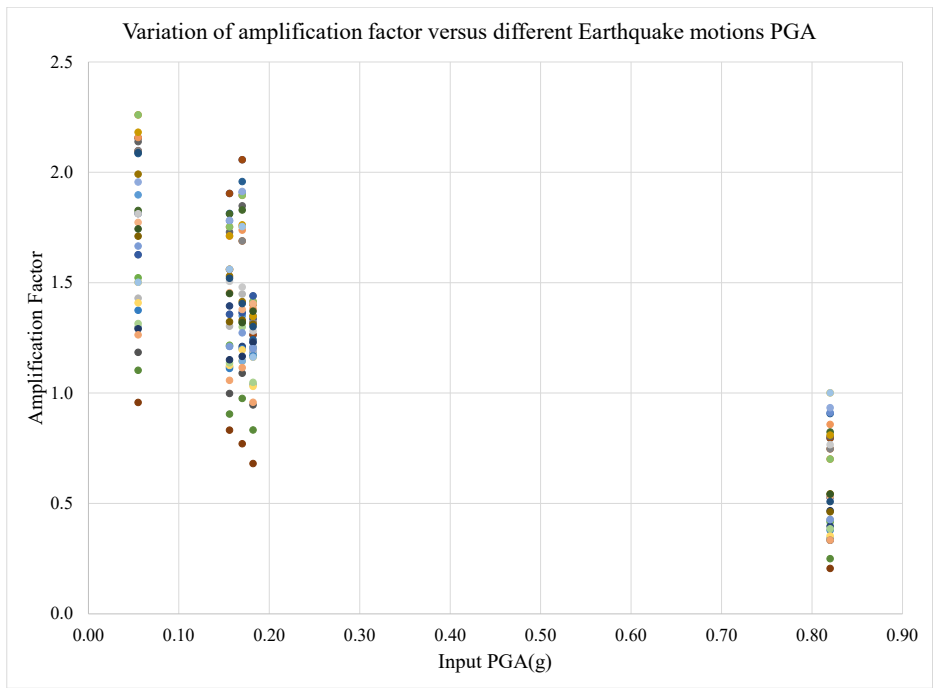

Figure 4.2: Variation of AF vs Input PGA for all the locations

Highlighting a varied response of the soil layers to the Kobe earthquake, i.e., in the extreme case of a high PGA of 0.82g, the amplification factors ranged from 0.205 to 1.001 across the different locations. This variability underscores the complex nature of the soil's reaction to the strong seismic waves generated by the Kobe earthquake motions. Similarly, for the Chi-Chi earthquake motion and the Loma Gilroy earthquake motion, both with moderate PGA values of 0.18g and 0.17g, respectively, the amplification factors demonstrated a range of 0.681 to 1.44 and 0.770 to 2.057.

4.3 Correlation between Amplification Factors and Soil Lithology

4.3.1 Maximum Amplification case

In examining the correlation between amplification factors and soil lithology for the five earthquake motions, notable patterns emerged in the maximum amplification case. The maximum amplification factor was observed at specific locations such as Balaju (BH-K4) for the Gorkha and Lima Gilroy earthquake motions, Shorakhutte (BH-K13) for the Aftershocks motion, Lazimpat (BH-K14) for the Chi-Chi earthquake motion, and Kumaripati (BH-L4) for the Kobe earthquake motion. These five specific locations' lithological characteristics were carefully studied and illustrated in figure 4.3 for Balaju (BH-K4), figure 4.4 for Shorakhutte (BH-K13), figure for 4.5 Lazimpat (BH-K14), and figure 4.6 for Kumaripati (BH-L4).

These findings offer insights into the intricate relationship between soil composition and the amplification response in different seismic scenarios. This suggests that the dark grey, loose soil may increase seismic ground motion amplification. It aligns with the understanding that certain soil types, particularly loose and potentially saturated soils, can lead to greater amplification during earthquake motion having moderate PGAs and Soil types with dense silty gravels including boulders, cobbles and pebbles, can lead to higher amplification during earthquake motion having higher PGA.

The clarity with which multiple soil layers respond to seismic motion is further enhanced by Figures 4.7 and 4.8, which provide an extensive overview of the dynamics of amplification in the locations under study. The statistics' distinctive patterns aid in improving the understanding of the changes in seismic site response across various lithological strata.
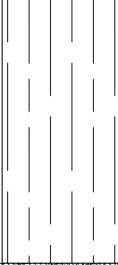
Depth (m)	Thickness (m)	Soil classification	Group Symbol	Soil Symbol
0 0.3	0.3	Filling Materials		
1.5	1.2	Gray loose silty sand	SM	
4	2.5	Black soft clayey silt of low plasticity	ML	
9.6	5.6	Gray loose miciasious silty fine sand	SM	
10.0	0.4	Black soft clayey silt of medium plasticity	ML	

Figure 4.3: Soil profile of Balaju (BH-K4)

4.3.2   Minimum Amplification case

In the case of minimum amplification, all five different earthquake motions consistently resulted in the same specific location, namely, Hariharbhawan (BH-L7). The lithological characteristic of Haribharbhawan (BH-L7) is illustrated in figure 4.9.

The variation of amplification factors along the depth of the location Hariharbhawan (BH-L7) is depicted in figure 4.10.

It is notable that between depths of 7m to 10m, there is a significant decrease in the amplification factor. To provide a comprehensive understanding of the dynamics of amplification, the shear wave velocity profile along with depth is studied, as

24
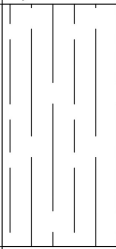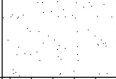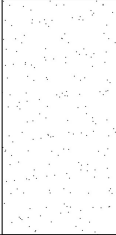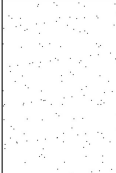
Depth (m)	Thickness (m)	Soil classification	Group Symbol	Soil Symbol
0 3.4	3.4	Filing materials including sandy silt with traces of pebbles	M	
4.5	1.10	Gray medium silty sand with gravels & pebbles	SP	
6.0	1.5	Dark gray medium clayey silt of low plasticity	ML	
9.3	3.3	Gray to white medium silty sand with gravels & pebbles	SP	
12.50	3.2	Gray to brown dense sandy gravels with traces of silt	GW	
15.0	2.5	Dark gray medium dense silty sand with traces of pebbles	SP	

Figure 4.4: Soil profile of Shorakhutte (BH-K13)

illustrated in figure 4.11. This low shear wave velocity range coincides with the substantial decrease in amplification factors at the same depths. So, this might be one of the reasons for the low amplification factors.

4.4 Spectral Acceleration (S_a)

In geotechnical earthquake engineering, spectral acceleration analysis is an essential tool for determining a region's seismic vulnerability and the potential effects on infrastructure. The significance of spectral acceleration analysis is made especially clear in this study, which concentrated on the ground response analysis of the
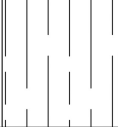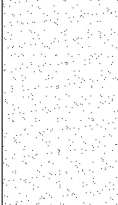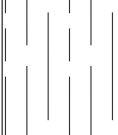
Depth (m)	Thickness (m)	Soil classification	Group Symbol	Soil Symbol
0 0.3	0.9	Vegetable top soil		
2.9	2.40	Gray to yellow medium uniform sandy silt	ML	
6.80	3.90	Dark gray medium well graded gravelly sand	SW	
10.90	4.10	Gray to white loose to medium uniform silty sand with traces of gravels	SM	
13.50	2.60	Dark gray medium uniform sandy silt	ML	
20	6.50	Dark gray medium well graded gravelly coarse to medium sand	SW	

Figure 4.5: Soil profile of Lazimpat (BH-K14)

Kathmandu Valley. For the valley to be seismically resilient, it is crucial to understand how ground motion varies across different time periods during an earthquake event. The ability to understand this complex relationship between ground motion and time periods is provided by spectral acceleration analysis, which enables us to identify the unique vulnerabilities and requirements that Kathmandu's geological and geotechnical characteristics impose during seismic events. The spectral acceleration outcomes for specific locations were compared with the criteria outlined in the Indian Standard Seismic Code (IS 1893 2016) and the Nepal Building Code (NBC 105 2020). Soft soil and very soft soil classifications were considered based on IS 1893 2016 and NBC 105 2020, respectively, incorporating a 5% damping ratio.

Depth (m)	Thickness (m)	Soil classification	Group Symbol	Soil Symbol
0	1.25	Filing materials		
1.25				
	13.75	Brown gray to white dense silty gravels including boulders, cobbles, pebbles and silt	GM	
15.0				

Figure 4.6: Soil profile of Kumaripati (BH-L4)

The comparison of spectral acceleration from IS 1893 2016, NBC 105 2020, input ground motion (Gorkha earthquake 2015), and ground surface acceleration spectrum of Balaju (BH-K4) is shown in figure 4.12. The maximum spectral acceleration obtained was 1.178g with a fundamental period of 0.269 sec.

The comparison of spectral acceleration from IS 1893 2016, NBC 105 2019, input ground motion (Gorkha earthquake 2015) and ground surface acceleration spectrum of Sorakhutte(BH-K13) is shown in figure 4.13. The maximum spectral acceleration obtained was 1.147g with a fundamental period of 0.269 sec.

The comparison of spectral acceleration from IS 1893 2016, NBC 105 2020, input ground motion (Gorkha earthquake 2015) and ground surface acceleration spectrum of Lazimpat(BH-K14) is shown in figure 4.14. The maximum spectral acceleration obtained was 0.828g with a fundamental period of 0.325 sec.

The comparison of spectral acceleration from IS 1893 2016, NBC 105 2020, input ground motion (Gorkha earthquake 2015) and ground surface acceleration spectrum of Kumaripati (BH-L4) is shown in figure 4.15. The maximum spectral acceleration obtained was 0.906g with a fundamental period of 0.253 sec.

The comparison of spectral acceleration from IS 1893 2016, NBC 105 2020, input ground motion (Gorkha earthquake 2015) and ground surface acceleration spectrum of Hariharbhawan (BH-L7) is shown in figure 4.16. The maximum spectral acceleration obtained was 0.373g with a fundamental period of 0.534 sec.

4.5   Interpretation and Validation of Results

One of the most intriguing findings of this analysis is the relationship between amplification factors (AF) and peak ground acceleration (PGA). The amplification factors (AF) observed across the study can be validated from the study of (A. Kumar et al., 2015)[41]. The finding of (A. Kumar et al., 2015)[41] concluded that the rate of change in amplification factor is found to be very high for PHA<0.08g, intermediate for 0.08g<PHA<0.22g and low for PHA>0.22g as illustrated in figure 4.17. So, the present study aligns with the findings of (A. Kumar et al., 2015)[41].

Specifically, higher values of AF are consistently associated with very low PGA values, as exemplified by the case of Aftershocks acceleration motion with a PGA of 0.055g. High AF for ground motions with low PHA are the attributes of nonlinear soil behaviour [41]. A study by (Bazzurro & Cornell, 2004)[42] on uncertain soil properties reveals that nonlinear soil behaviour can cause substantial amplification of ground-motion intensity at longer oscillator periods. So, the observation of higher amplification factors (AF) corresponding to very low values of peak ground acceleration (PGA), as exemplified by the case of aftershocks with a PGA of 0.055g, finds validation in prior research. The Amplification factors range observed using the aftershock, 0.958 to 2.26, indicates a substantial amplification. The study of (A. Kumar et al., 2015)[41] supports this finding, as they noted that the rate of change in amplification factor is very high for PHA values below 0.08g as shown in figure 4.17 which aligns with current findings and reinforces the significance of these

observations. Similarly, large amplifications corresponding to low-amplitude ground motions reported above were also observed during the 1989 Loma Prieta earthquake and 1985 Michoacan earthquakes, as reported by (Romero, 2001)[43].

The AF range observed using the Kobe earthquake motion with a PGA of 0.82g, 0.205 to 1.001, indicates a reduced amplification effect. This result can be validated by the study of (Romero, 2001)[43]. According to (Romero, 2001), substantial accelerations are associated with significant strains. The soil's behavior at large strains is primarily influenced by its exceptionally high damping ratio, leading to minimal amplification in ground motion compared to input motions with lower acceleration[41]. The change in amplification factor is low for PHA values above 0.22g as shown in figure 4.17 which supports the finding that low amplification factors (AF) correspond to very high values of peak ground acceleration (PGA), as exemplified by the case of Kobe earthquake motion with a PGA of 0.82g, which finds validation in prior research.
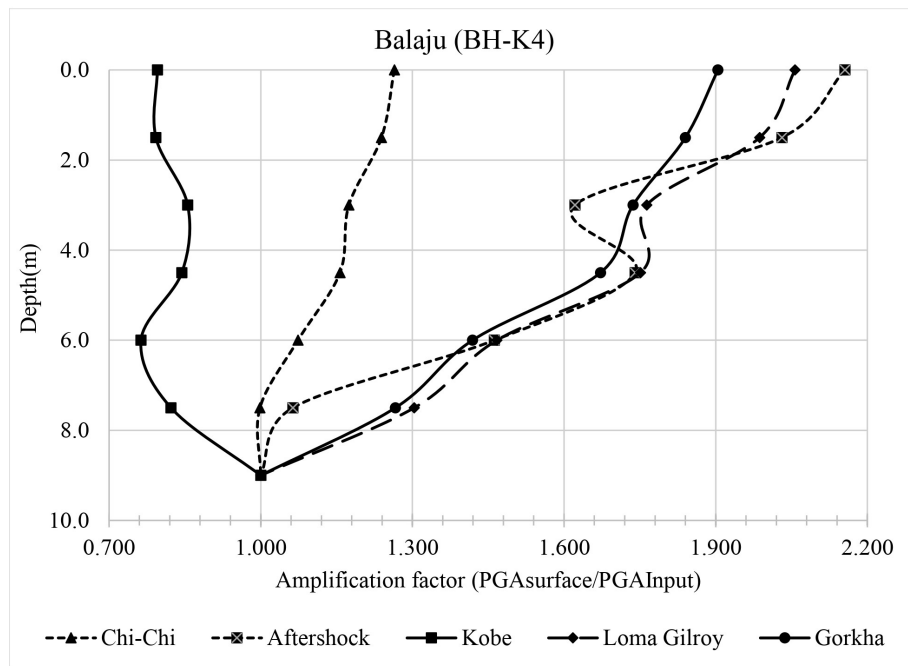
(a)
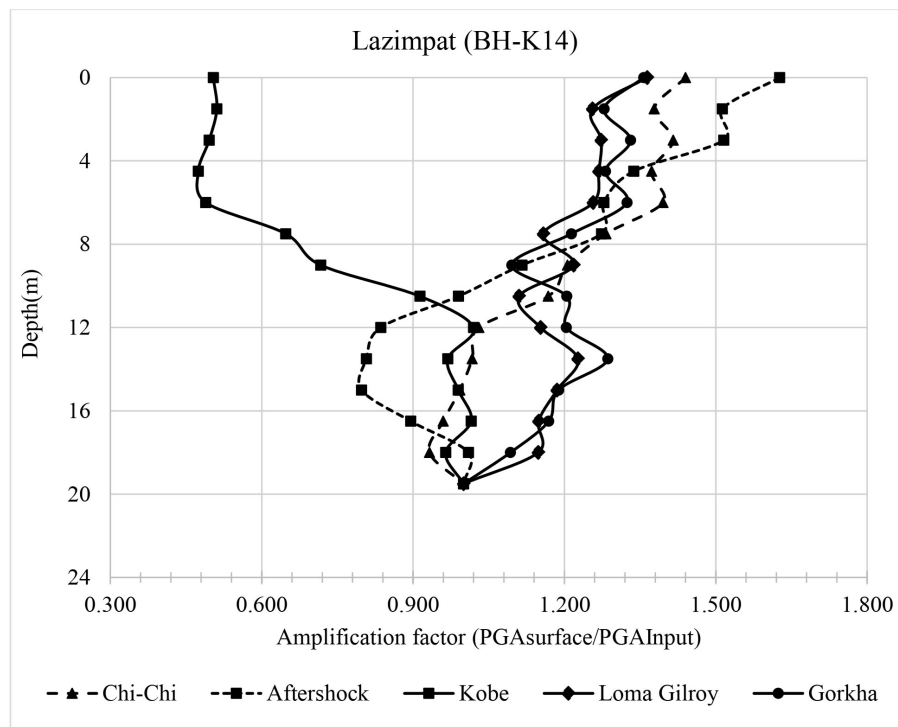
(b)

Figure 4.7: (a),(b): Variation of Amplification factor V/s depth at Balaju and Lazimpat
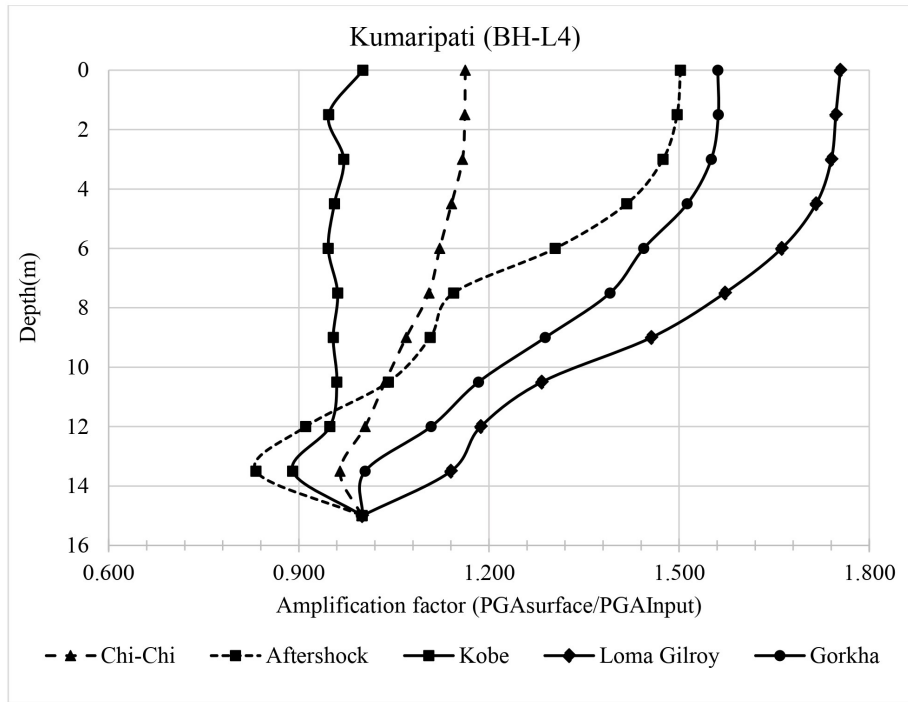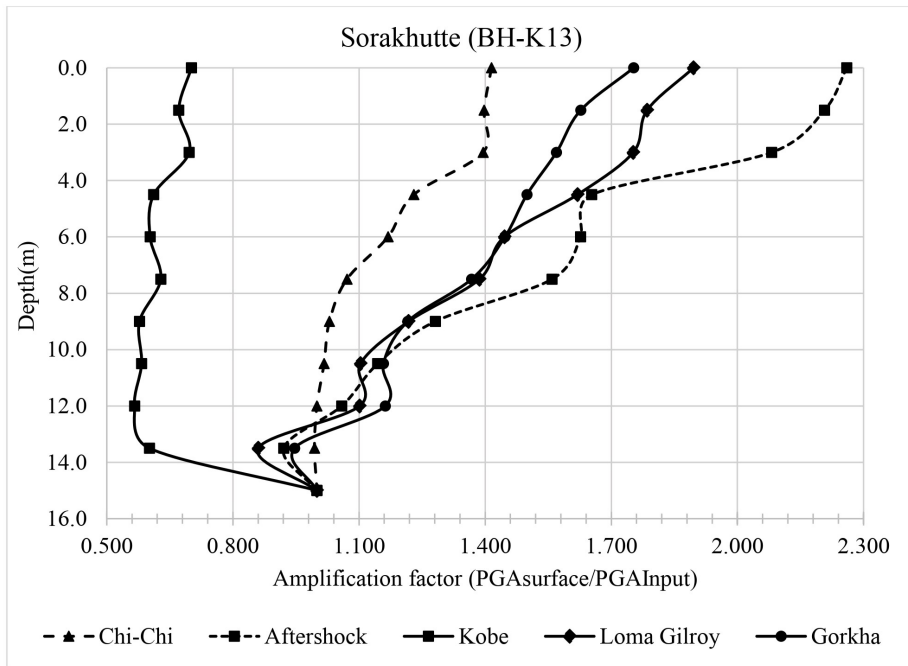
Figure 4.8: (a),(b): Variation of Amplification factor V/s depth at Kumaripati anns Sorakhutte

Depth (m)	Thickness (m)	Soil classification	Group Symbol	Soil Symbol
0	0.9	Filing materials		
0.9				
1.8	0.9	Light gray to brown medium clayey silt of low plasticity including traces of pebbles	ML	
15.0	13.2	Light gray very soft to medium clayey silt of low plasticity	ML	

Figure 4.9: Soil profile of Hariharbhawan (BH-L7
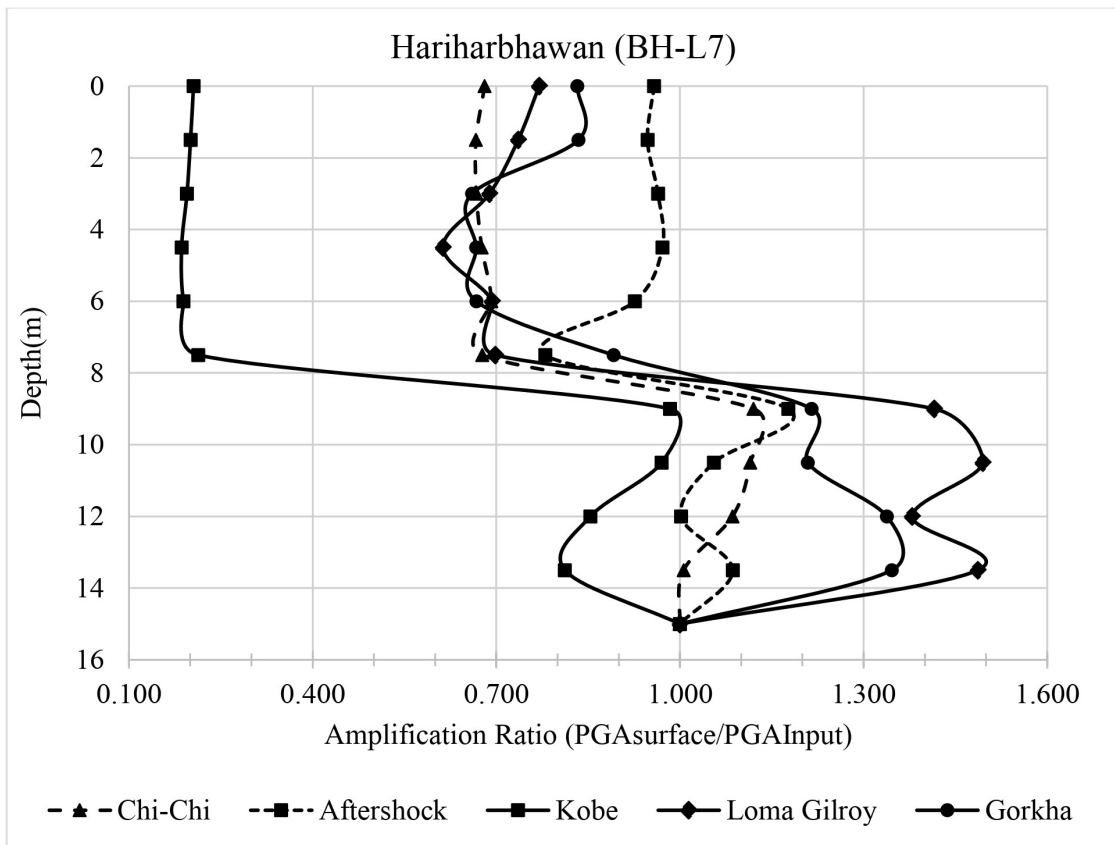
Figure 4.10: Variation of Amplification factor Vs depth
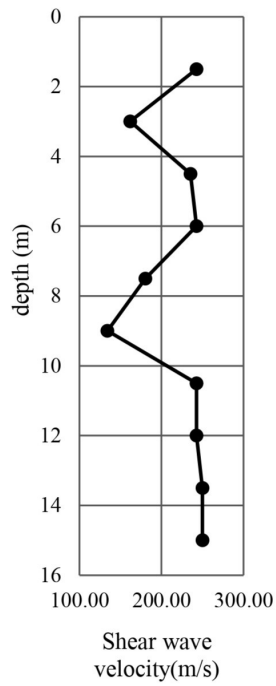
Figure 4.11: Variation of Shear wave velocity along with depth at Hariharbhawan (BH-L7)
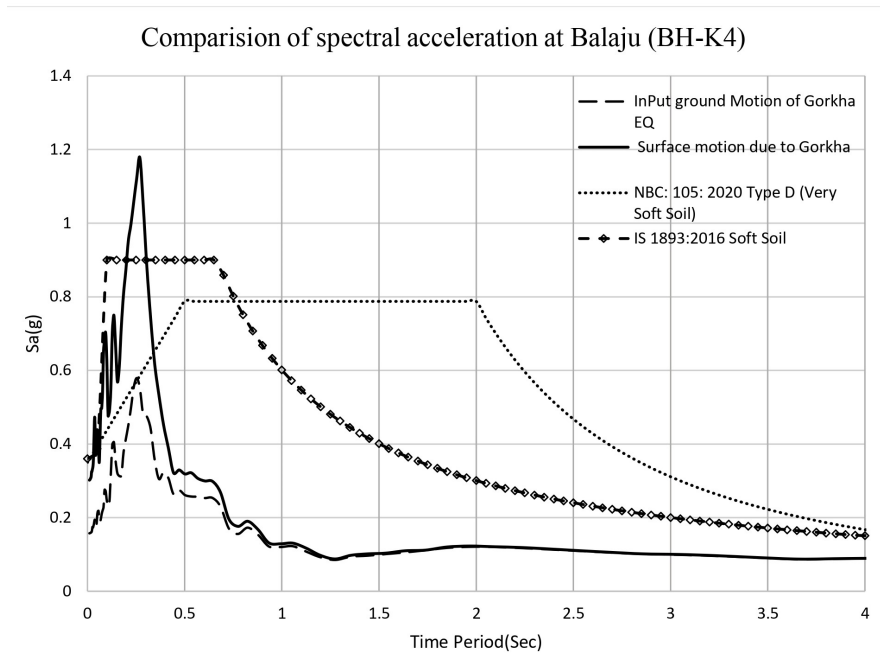
Figure 4.12: Comparison of obtained response spectra from Gorkha Earthquake as input motion with code provision at Balaju (BH-K4)
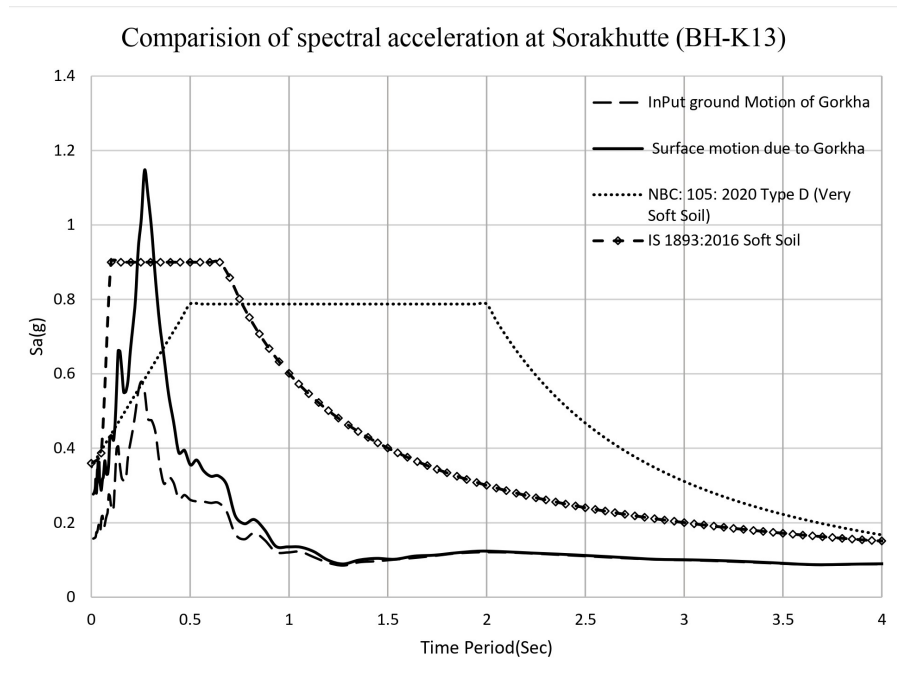
Figure 4.13: Comparison of obtained response spectra from Gorkha Earthquake as input motion with code provision at Sorakhutte (BH-K13)
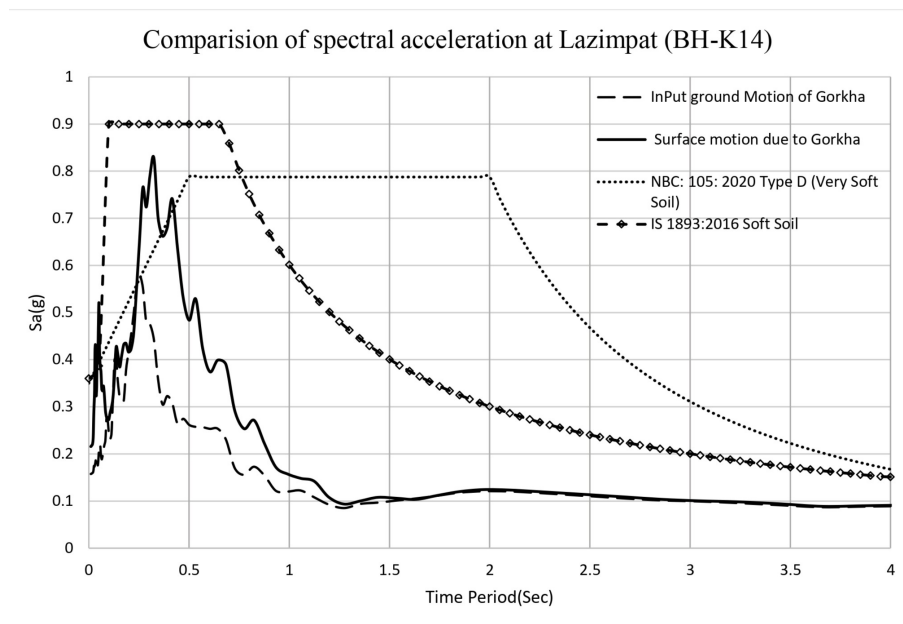
Figure 4.14: Comparison of obtained response spectra from Gorkha Earthquake as input motion with code provision at Lazimpat (BH-L7)
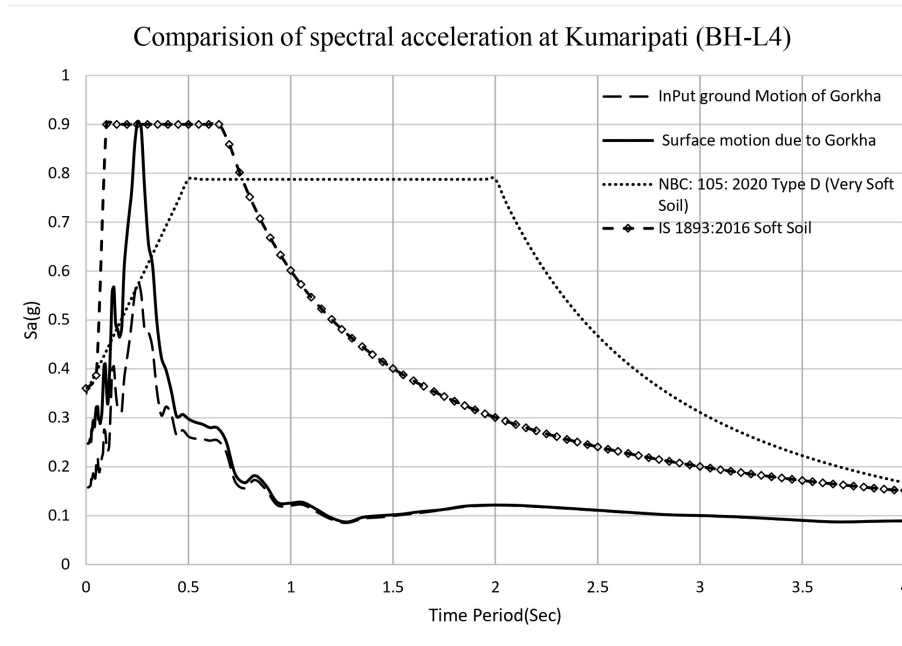
Figure 4.15: Comparison of obtained response spectra from Gorkha Earthquake as input motion with code provision at Kumaripati (BH-L4)
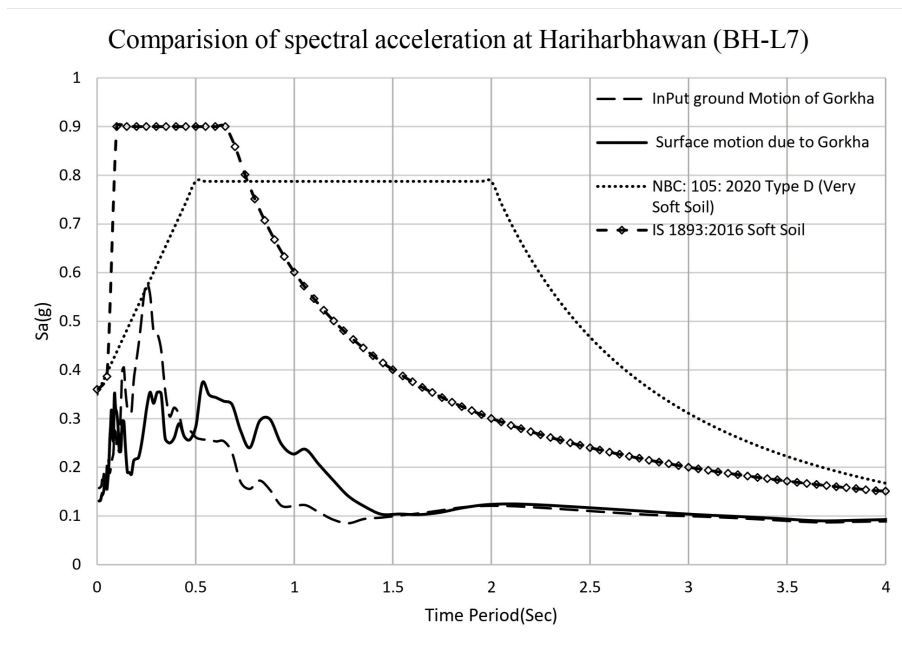
Figure 4.16: Comparison of obtained response spectra from Gorkha Earthquake as input motion with code provision at Hariharbhawan(BH-L7)
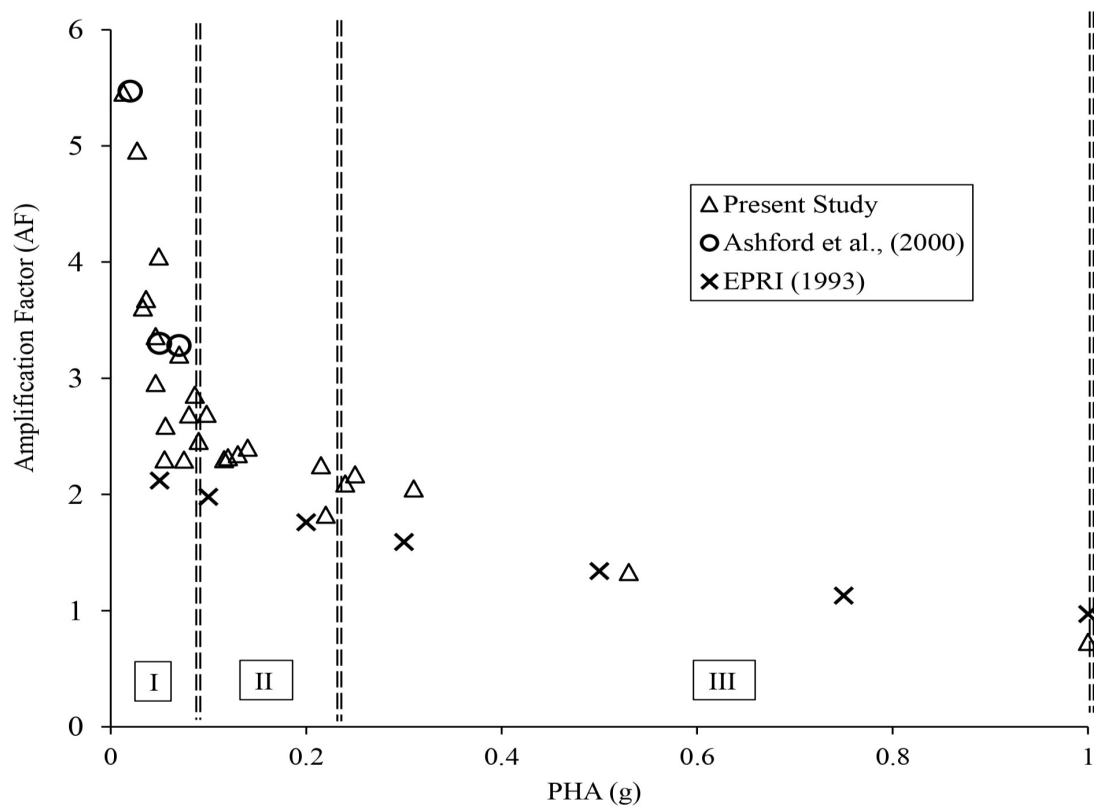
Figure 4.17: Variation of amplification factor versus PHA[41]

CHAPTER FIVE:CONCLUSION

The complex relationship between soil type and amplification factors (AF) is a well-recognized aspect of seismic site response analysis. In this study, it was found that the site having a depth of dark grey loose soil resulted in higher AF. The observation also aligns with the findings of [44], who identified Balaju as one of the areas in the Kathmandu Valley with concentrated damage during the Gorkha earthquake. Based on the Soil profile of Balaju (BH-k4) as shown in figure 4.7a, it is evident that the amplification of ground is primarily due to the properties of the grey loose micaceous silty fine sand. The higher amplification at Balaju is due to the young, unconsolidated fine sand, which results from alluvium deposition of the river [12]. The following conclusion can be drawn:

- Local geology plays a pivotal role in influencing the amplification of ground responses during different seismic events.

- The study evaluates how the soil reaction depends not only on the soil type but also on the different earthquake input motions, shear wave velocity, density, frequency, and characteristics of the soil or rock layer.

- While high amplification factors (AF) suggest soil response variations, it is crucial to contextualize them within standard seismic codes. Even if a site has a high AF, it may not necessarily result in significant harm if the response spectra fall within the acceptable limits prescribed by standard seismic codes.

- Furthermore, seismic micro-zonation relies heavily on amplification factors, which are crucial in earthquake risk analysis and sustainable development planning. However, focusing solely on amplification factors for micro-zonation is an incomplete approach.

REFERENCES

[1] A. Renton, "Climate change is triggering "extreme geological events", like the nepal earthquake," Apr 2015. [Online]. Available: https://stiffupperlip.org.uk/2015/04/28/climate-change-is-triggering-extreme-geological-events-like-the-nepal-earthquake/

[2] A. Dixit, L. Dwelley-Samant, M. Nakarmi, S. B. Pradhanang, and B. Tucker, "The kathmandu valley earthquake risk management project: an evaluation," *Asia Disaster Preparedness Centre: http://www. iitk. ac. in/nicee/wcee/article/0788. pdf*, 2000.

[3] T. B. Gaha, B. Bhusal, S. Paudel, and S. Saru, "Investigation of ground response analysis for kathmandu valley: a case study of gorkha earthquake," *Arabian Journal of Geosciences*, vol. 15, no. 15, p. 1354, 2022.

[4] P. N. Maskey and T. Datta, "Risk consistent response spectrum and hazard curve for a typical location of kathmandu valley," in *13th World Conference on Earthquake Engineering paper no*, vol. 3124, 2004.

[5] Y. Paudyal, N. Bhandary, and R. Yatabe, "Seismic microzonation of densely populated area of kathmandu valley of nepal using microtremor observations," *Journal of Earthquake Engineering*, vol. 16, no. 8, pp. 1208–1229, 2012.

[6] Y. Igarashi and M. Yoshida, "History of vegetation and climate in the kathmandu valley," 1988.

[7] H. Sakai, R. Fujii, Y. Kuwahara, B. N. Upreti, and S. D. Shrestha, "Core drilling of the basin-fill sediments in the kathmandu valley for palaeoclimatic study: preliminary results," *Journal of Nepal Geological Society*, vol. 25, p. 9, 2001.

[8] M. Yoshida, "Neogene to quartenery lacustrine sediments in the kathmandu valley, nepal." *Journal of Nepal Geological Society, Special Issue*, vol. 4, pp. 73–100, 1984.

[9] S. Maharjan, A. Poujol, C. Martin, G. Ameri, D. Baumont, K. Hashemy, Y. Benjelloun, and H. Shible, "New probabilistic seismic hazard model for nepal himalayas integrating distributed seismicity and major thrust faults," 2023.

[10] Y. R. Paudyal, R. Yatabe, N. P. Bhandary, and R. K. Dahal, "Basement topography of the kathmandu basin using microtremor observation," *Journal of Asian Earth Sciences*, vol. 62, pp. 627–637, 2013.

[11] G. Chitrakar and M. R. Pandey, "Historical earthquakes of nepal," *Bull. Geol. Soc. Nepal*, vol. 4, pp. 7–8, 1986.

[12] K. Sharma, M. Subedi, R. R. Parajuli, and B. Pokharel, "Effects of surface geology and topography on the damage severity during the 2015 nepal gorkha earthquake," *Lowland Technology International*, vol. 18, no. 4, March, pp. 269–282, 2017.

[13] A. Johari and S. Pourbeirak, "Stochastic site response analysis of sandy soil by random finite difference method."

[14] M. Rayhani, M. El Naggar, and S. Tabatabaei, "Nonlinear analysis of local site effects on seismic ground response in the bam earthquake," *Geotechnical and Geological Engineering*, vol. 26, pp. 91–100, 2008.

[15] S. E. Hough, J. R. Altidor, D. Anglade, D. Given, M. G. Janvier, J. Z. Maharrey, M. Meremonte, B. S.-L. Mildor, C. Prepetit, and A. Yong, "Localized damage caused by topographic amplification during the 2010 m 7.0 haiti earthquake," *Nature Geoscience*, vol. 3, no. 11, pp. 778–782, 2010.

[16] M. Celebi, "Topographical and geological amplifications determined from strong-motion and aftershock records of the 3 march 1985 chile earthquake," *Bulletin of the Seismological Society of America*, vol. 77, no. 4, pp. 1147–1167, 1987.

[17] C.-H. Loh, Z.-K. Lee, T.-C. Wu, and S.-Y. Peng, "Ground motion characteristics of the chi-chi earthquake of 21 september 1999," *Earthquake engineering & structural dynamics*, vol. 29, no. 6, pp. 867–897, 2000.

[18] K. Aki, "Local site effects on weak and strong ground motion," *Tectonophysics*, vol. 218, no. 1-3, pp. 93–111, 1993.

[19] S. E. Hough and B. Roger, "Site response of the ganges basin inferred from re-evaluated macroseismic observations from the 1897 shillong, 1905 kangra,

and 1934 nepal earthquakes," *Journal of Earth System Science*, vol. 117, pp. 773–782, 2008.

[20] M. Pandey and P. Molnar, "The distribution of intensity of the bihar-nepal earthquake of 15 january 1934 and bounds on the extent of the rupture zone," *Journal of Nepal Geological Society*, vol. 5, no. 1, p. 22, 1988.

[21] J.-L. Mugnier, P. Huyghe, A. P. Gajurel, B. N. Upreti, and F. Jouanne, "Seismites in the kathmandu basin and seismic hazard in central himalaya," *Tectonophysics*, vol. 509, no. 1-2, pp. 33–49, 2011.

[22] M. R. Pandey, "Ground response of kathmandu valley on the basis of microtremors," in *Proceedings of the 12th world conference on earthquake engineering, Auckland, New Zealand*, vol. 30, 2000.

[23] C. K. Kawan, P. N. Maskey, and G. B. Motra, "A study of local soil effect on the earthquake ground motion in bhaktapur city, nepal using equivalent linear and non-linear analysis," *Iranian Journal of Science and Technology, Transactions of Civil Engineering*, vol. 46, no. 6, pp. 4481–4498, 2022.

[24] S. S. Kumar, P. Acharya, P. K. Dammala, and M. K. Adapa, "Characterization of ground response and liquefaction for kathmandu city based on 2015 earthquake using total stress and effective stress approach," *International Journal of Geotechnical Earthquake Engineering (IJGEE)*, vol. 11, no. 2, pp. 1–25, 2020.

[25] D. Gautam, H. Chaulagain, H. Rodrigues, and H. R. Shahi, "Ground response based preliminary microzonation of kathmandu valley," *Geotech. Eng*, vol. 48, pp. 87–92, 2017.

[26] A. Kumar, N. Harinarayan, and O. Baro, "Nonlinear soil response to ground motions during different earthquakes in nepal, to arrive at surface response spectra," *Natural Hazards*, vol. 87, pp. 13–33, 2017.

[27] N. Puri, A. Jain, P. Mohanty, and S. Bhattacharya, "Earthquake response analysis of sites in state of haryana using deepsoil software, proced. comput. sci., 125, 357–366," 2018.

[28] J. Krahenbuhl and A. Wagner, "Survey, design, and construction of trail suspension bridges for remote areas, skat," *Swiss Center for Appropriate Technology in St. Gallen, Switzerland*, 1983.

[29] S. MORIBAYASHI and Y. MARUO, "Basement topography of the kathmandu valley, nepal an application of gravitational method to the survey of a tectonic basin in the himalayas," *Journal of the Japan Society of Engineering Geology*, vol. 21, no. 2, pp. 80–87, 1980.

[30] Y. Maruo, S. Moribayashi, and R. Tandukar, "Gravity map of kathmandu valley," *Institute for International Cooperation, JICA, Tokyo*, 1999.

[31] S. S. Karki and N. K. Tamrakar, "Fluvial morphology and dynamics of the godavari khola, southeast kathmandu, central nepal," *Bulletin of the Department of Geology*, vol. 19, pp. 15–28, 2016.

[32] Y. Ohta and N. Goto, "Empirical shear wave velocity equations in terms of characteristic soil indexes," *Earthquake engineering & structural dynamics*, vol. 6, no. 2, pp. 167–187, 1978.

[33] S. L. Kramer, *Geotechnical earthquake engineering.* Pearson Education India, 1996.

[34] R. L. Kondner, "A hyperbolic stressstrain formulation for sands," in *Proc. 2nd Pan-American Conf. on SMFE*, vol. 1, 1963, pp. 289–324.

[35] N. Matasović and M. Vucetic, "Cyclic characterization of liquefiable sands," *Journal of Geotechnical Engineering*, vol. 119, no. 11, pp. 1805–1822, 1993.

[36] Y. M. Hashash and D. Park, "Non-linear one-dimensional seismic ground motion propagation in the mississippi embayment," *Engineering Geology*, vol. 62, no. 1, pp. 185–206, 2001, earthquake hazard evaluation in the Central United States. [Online]. Available: https://www.sciencedirect.com/science/article/pii/S0013795201000618

[37] Y. Hashash, C. Phillips, and D. R. Groholski, "Recent advances in non-linear site response analysis," 2010.

[38] G. MASING, "Eigenspannungen und verfestigung beim messing," in *Proceedings, second international congress of applied mechanics*, 1926, pp. 332–335.

[39] M. Vucetic and R. Dobry, "Effect of soil plasticity on cyclic response," *Journal of geotechnical engineering*, vol. 117, no. 1, pp. 89–107, 1991.

[40] H. B. Seed, "Soil moduli and damping factors for dynamic response analyses," *Reoprt*, pp. EERC–70, 1970.

[41] A. Kumar, N. Harinarayan, and O. Baro, "High amplification factor for low amplitude ground motion: assessment for delhi," *Disaster Adv*, vol. 8, no. 12, pp. 1–11, 2015.

[42] P. Bazzurro and C. A. Cornell, "Ground-motion amplification in nonlinear soil sites with uncertain properties," *Bulletin of the Seismological Society of America*, vol. 94, no. 6, pp. 2090–2109, 2004.

[43] S. M. Romero, *Ground motion amplification of soils in the upper Mississippi embayment.* Georgia Institute of Technology, 2001.

[44] H. Hazarika, N. Bhandary, Y. Kajita, K. Kasama, K. Tsukahara, and R. Pokharel, "The 2015 nepal gorkha earthquake: An overview of the damage, lessons learned and challenges," *lowland technology international*, vol. 18, no. 2, Sep, pp. 119–128, 2016.

APPENDIX A: BOREHOLE LOG

					MULTI Lab (P) Ltd.				

<table>
<tr><td colspan="10" align="center">MULTI Lab (P) Ltd.
BORE HOLE LOG</td></tr>
<tr><td colspan="3">Project Name</td><td>:</td><td colspan="6">Soil Investigation of Proposed Building Site</td></tr>
<tr><td colspan="3">Location</td><td>:</td><td colspan="6">Ghatthaghat, Bhaktapur</td></tr>
<tr><td colspan="3">Bore Hole No</td><td>:</td><td colspan="6">1</td></tr>
<tr><td colspan="3">Diameter of BH, mm</td><td>:</td><td colspan="6">100mm</td></tr>
<tr><td colspan="3">RL of GWT, m</td><td>:</td><td colspan="6">5.50 m</td></tr>
<tr><td colspan="3">Date</td><td>:</td><td colspan="6">27th March, 2009</td></tr>
<tr><td colspan="3">Logged By</td><td>:</td><td colspan="6">Manoj Subedi</td></tr>
<tr><td colspan="3">Checked By</td><td>:</td><td colspan="6">Sandeep Kr. Jha</td></tr>
<tr><td colspan="3">Geotechnical Expert</td><td>:</td><td colspan="6">Dr. R. K. Poudel</td></tr>
</table>

Scale 1=0.5m Each	Depth m	Thickness m	Sampling Depth m	Sampling Type	Soil Classification	Group Symbol	Soil Symbol	SPT Value N
	0-0.40				Filling materials			
			1.50	SPT	Gray to brown soft clayey silt of low plasticity	ML		7
		2.60						
	3.00		3.00	SPT				8
		5.10	4.50	SPT	Gray soft silty sand	SP		12
	5.10							
		1.00			Yellow to brown medium to coarse sand with traces of pebbles	SW		
	6.10		6.00	SPT				7
			7.50	SPT				6
			9.00	SPT				6
		8.90	10.50	SPT	Dark gray soft clayey silt of low plasticity	ML		5
			12.00	SPT				6
			13.50	SPT				7
	15.00		15.00	SPT				6

Figure A.1: Borehole Log of gattaghar (BH-B2)

MULTI Lab (P) Ltd.
BORE HOLE LOG

Project Name	:	Soil Investigation of Proposed Oriental Building Complex
Location	:	Baneshwor, Kathmandu
Bore Hole No	:	**2**
Diameter of BH, mm	:	100mm
RL of GWT, m	:	3.50 m
Date	:	23rd Nov, 2008 to 24th Nov, 2008
Logged By	:	Manoj Subedi
Checked By	:	Sandeep Kr. Jha
Geotechnical Expert	:	Dr. R. K. Poudel

Scale 1=1m Each	Depth m	Thickness m	Sampling Depth m	Sampling Type	Soil Classification	Group Symbol	Soil Symbol	SPT Value N
	0-0.40				Filling Materials			
	1.50	1.10	1.50	SPT	Yellow to brown firm clayey silt of low plasticity	ML		8
	4.30	2.80	3.00	SPT	Dark gray medium sandy silt	SP		7
	5.50	1.20	4.50	SPT	Light gray medium coarse sand with traces of pebbles	SW		13
	7.30	1.80	6.00	SPT	Dark gray soft clayey silt of medium plasticity	MI		4
	10.10	2.80	7.50	SPT	Light gray coarse sand	SW		6
			9.00	SPT				13
	11.00	0.90	10.50	SPT	Dark gray clayey silt of low plasticity	ML		6
		6.30	12.00	SPT	Light gray medium coarse sand with traces of pebbles	SW		16
			13.50	SPT				17
	17.30		15.00	SPT				18
	22.00	4.70			Dark gray soft clayey silt with medium plasticity	MI		

Figure A.2: Borehole Log of New-Baneswor (BH-K3)

45

MULTI Lab (P) Ltd.
BORE HOLE LOG

Project Name	:	Balaju Housing
Location	:	Balaju, Kathmandu
Bore Hole No	:	2 (10m)
Diameter of BH, mm	:	100mm
Drilling Method	:	Wash
RL of GWT, m	:	4.0 m
Date	:	19th Dec, 2007
Nos. of Helper	:	5
Logged By	:	Manoj Subedi
Checked By	:	Sandeep Kr. Jha
Certified By	:	Dr. R. K. Poudel

Scale 1=25cm Each	Depth m	Thickness m	Sampling Depth m	Sampling Type	Soil Classification	Group Symbol	Soil Symbol	SPT Value N
	0-0.30				Filling Materials			
		1.20			Gray loose silty sand	SM		
	1.50		1.50	SPT				2
		2.50	3.00	SPT	Black soft clayey silt of low plasticity	ML		3
	4.00							
			4.50	SPT				9
			6.00	SPT				7
		5.60			Gray loose miciasious silty fine sand	SM		
			7.50	SPT				10
			9.00	SPT				9
	9.60							
	10.00	0.40			Black soft clayey silt of medium plasticity	MI		

Figure A.3: Borehole Log of Balaju (BH-K4)

46

MULTI Lab (P) Ltd.

BORE HOLE LOG

Project	:	**Soil Investigation of Proposed Hotel Tara Building Complex**
Location	:	**Maharajgunj, Kathmandu**
Client	:	**C.E Services Pvt. Ltd**
Bore Hole No	:	**1**
Diameter of BH, mm	:	100 m
RL of GWT	:	3.50 m
Date	:	11th Nov 2010
Logged By	:	Ganesh Karki
Prepared By	:	Manoj Subedi
Checked By	:	Sandeep Kr. Jha
Certified By	:	Dr. R. K. Poudel

Scale 1=50cm Each	Depth m	Thickness m	Sampling Depth m	Type	Soil Classification	Group Symbol	Soil Symbol	SPT (Field Record) 15 cm	30 cm	45 cm	Value N
	0-0.50				Vegetable top soil						
	2.00	1.50	1.50	SPT	Light gray medium sandy silt	M		2	3	3	**6**
	3.00	1.00			Gray to white medium medium to coarse sand with pebbles	SW					
			3.00	SPT				4	3	5	**8**
			4.50	SPT				4	4	5	**9**
		4.50	5.00	UDS	Light gray medium silt of low plasticity & some cut layer of silty sand	M					
			6.00	SPT				4	5	4	**9**
	7.50										
			7.50	SPT				7	10	8	**18**
			9.00	SPT				10	11	10	**21**
			10.50	SPT				12	12	10	**22**
		12.50	12.00	SPT	Gray to white medium medium to fine sand with traces of pebbles	SW		9	10	12	**22**
			13.50	SPT				8	13	10	**23**
	15.00		15.00	SPT				8	14	11	**25**

Figure A.4: Borehole Log of Maharajung (BH-K5)

MULTI Lab (P) Ltd.
BORE HOLE LOG

Project Name	:	Soil Investigation of Proposed Birendra Maharjan's Building Site
Location	:	Kumaripati , Lalitpur
Bore Hole No	:	**1**
Diameter of BH, mm	:	100
RL of GWT, m	:	12.0 m
Date	:	6th June to 10th June, 2009
No. of Helper	:	5
Dirller's Name	:	Rajan Magar
Logged by	:	Ram Kumar Yadav
Drilling Suppervisor's Name	:	S. K. Jha
Geotechnical Expert	:	Dr. R. K. Poudel

Scale 1=50cm Each	Depth m	Thickness m	Sampling Depth m	Sampling Type	Soil Classification	Group Symbol	Soil Symbol	SPT Value N
	0.00				Filing Materials			
	1.25							
			1.50	SPT				**>50**
			3.00	SPT				**>50**
			4.50	SPT				**>50**
			6.00	SPT				**>50**
			7.50	SPT				**>50**
		14.55	9.00	SPT	Brown gray to white dense silty gravels including boulders, cobbles, pebbles and silt	GM		**>50**
			10.50	SPT				**>50**
			12.00	SPT				**>50**
			13.50	SPT				**>50**
			15.00	SPT				**>50**
	15.80							
			16.50					**30**
		4.20	18.00		Gray to brown medium dense sandy silt including silt & traces of gravels & pebbles	M		**32**
			19.50					**30**
	20.00							

Figure A.5: Borehole Log of Kumaripati (BH-L4)

MULTI Lab (P) Ltd.
BORE HOLE LOG

Project Name	:	Proposed Central Office Building For Karmachari Sanchaya Kosh
Location	:	Harihar Bhawan, Pulchowk
Bore Hole No	:	**2**
Consultant	:	**Araniko Designers & Planners**
Diameter of BH, mm	:	100mm
RL of GWT, m	:	1.70 m
Date	:	1st June to 2nd June, 2009
Logged By	:	Manoj Subedi
Checked By	:	Sandeep Kr. Jha
Geotechnical Expert	:	Dr. R. K. Poudel

Scale 1=0.5m Each	Depth m	Thickness m	Sampling Depth m	Sampling Type	Soil Classification	Group Symbol	Soil Symbol	SPT Value N
	0.00				Filling materials			
	0.90							
		0.90	1.50	SPT	Light gray to brown medium clayey silt of low plasticity including traces of pebbles	ML		9
	1.80							
			3.00	SPT				2
			4.50	SPT				8
			6.00	SPT				9
			7.00	UDS				
			7.50	SPT				3
		13.20	9.00	SPT	Light gray very soft to medium clayey silt of low plasticity	ML		1
			10.50	SPT				9
			12.00	SPT				9
			13.50	SPT				10
	15.00		15.00	SPT				10

Figure A.6: Borehole Log of hariharbhawan (BH-L7)

49

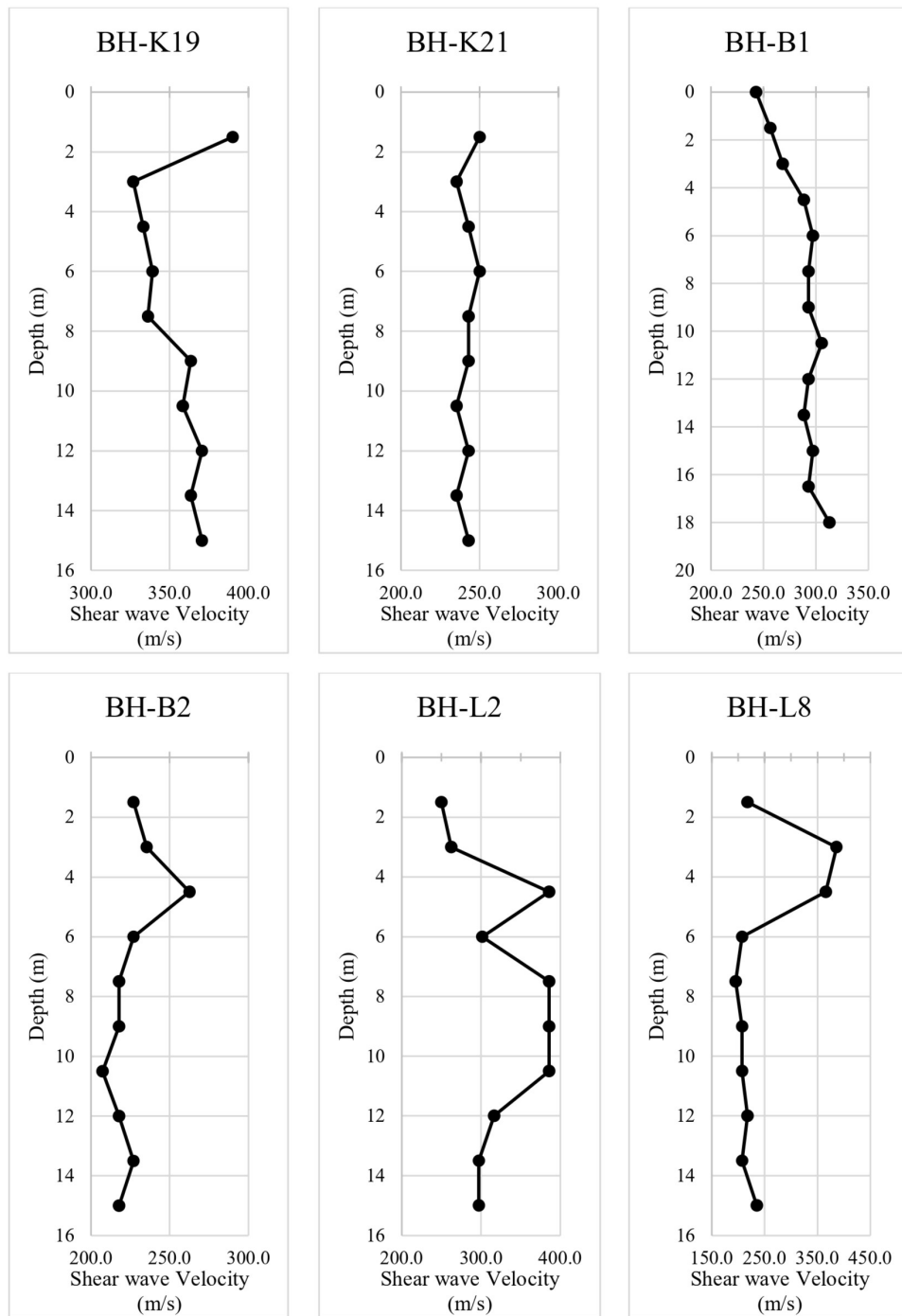# APPENDIX B: SHEARWAVE VELOCITY PROFILE

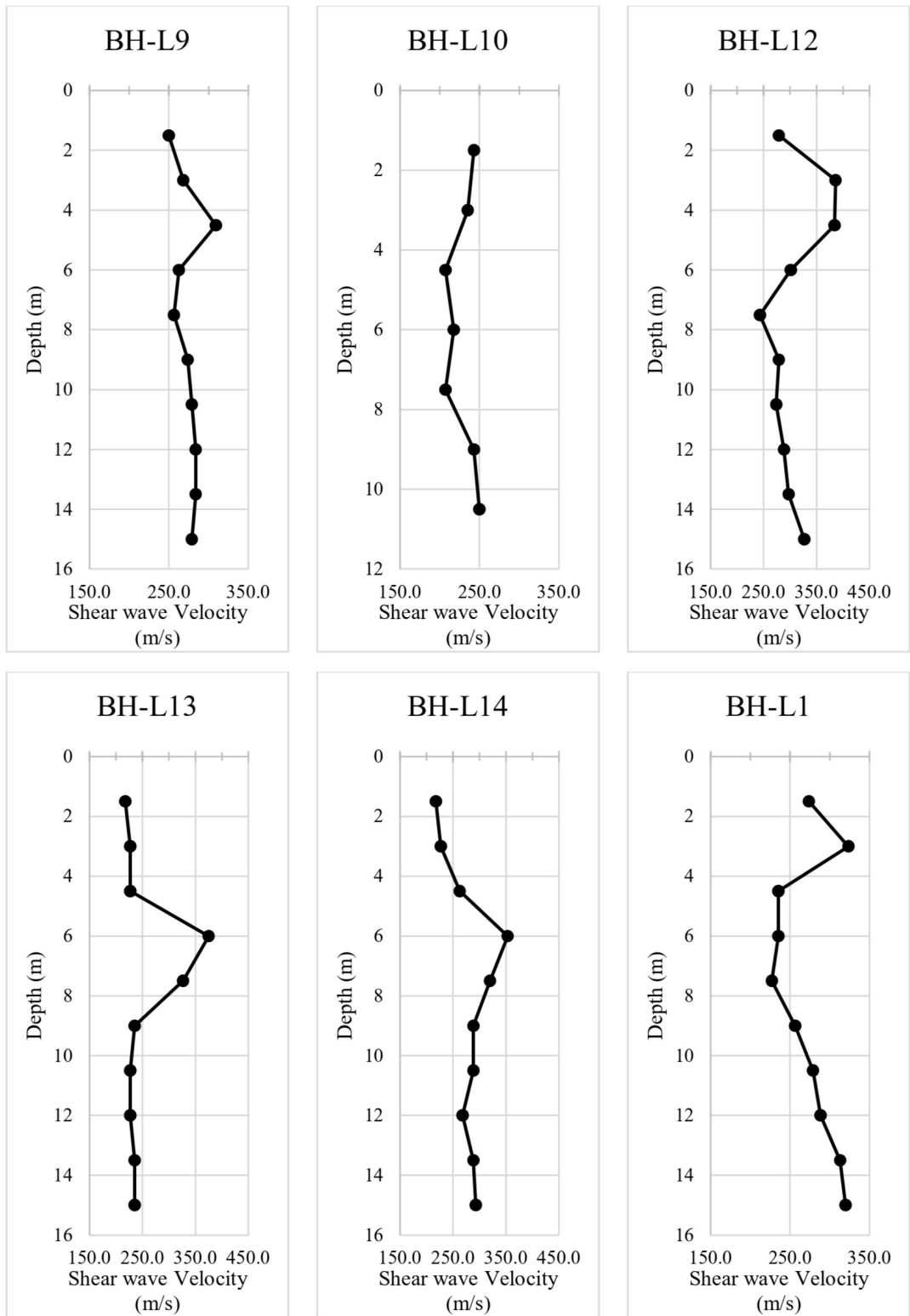

Figure A.7: Variation of Shearwave velocity across depth

Figure A.8: Variation of Shearwave velocity across depth
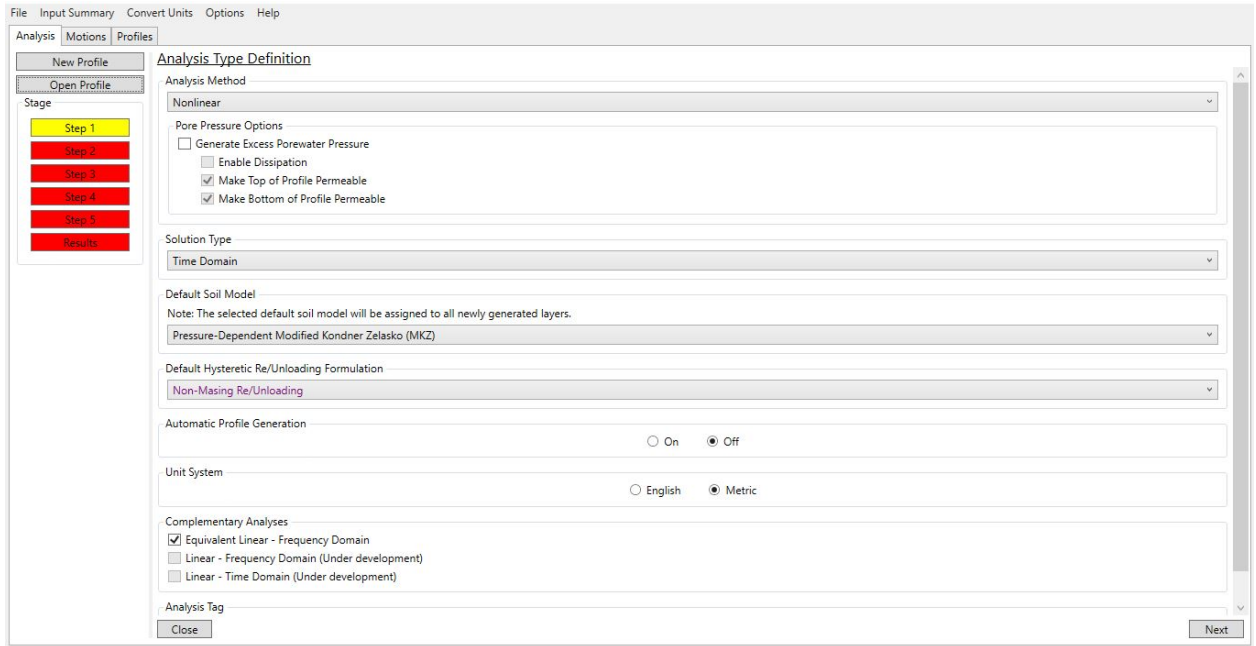
51

APPENDIX C: DEEPSOIL MODELLING

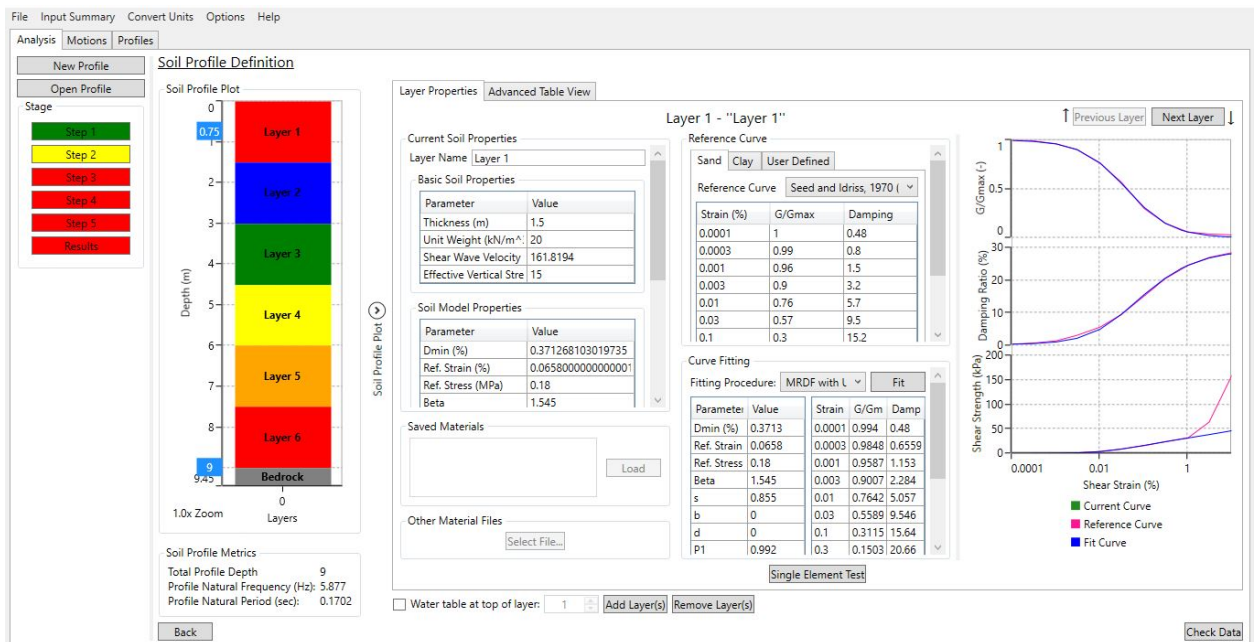**Figure A.9:** Step 1:Analysis Type Definition
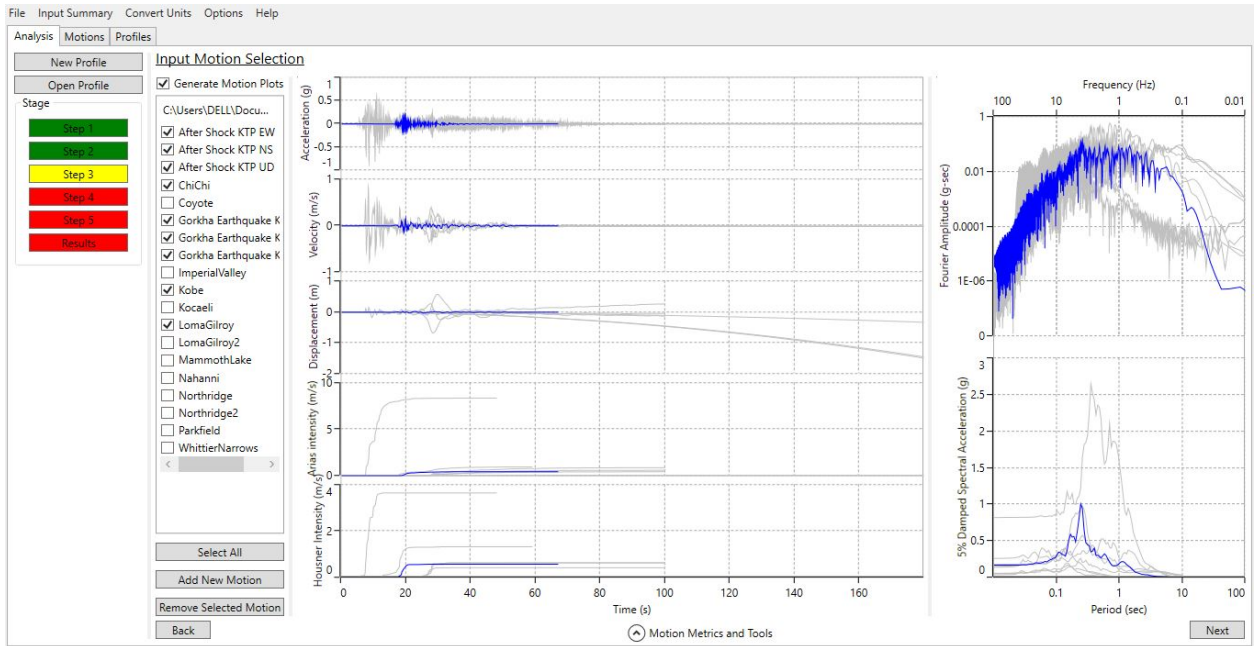

Figure A.10: Step 2:Soil Profile Definition
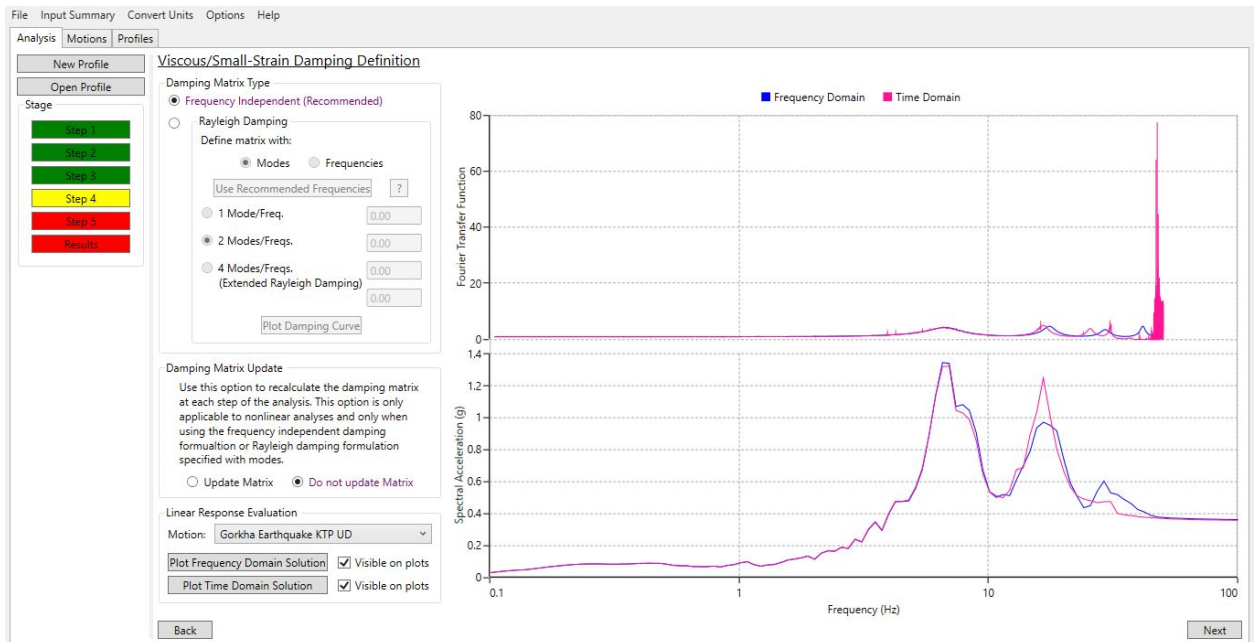
Figure A.11: Step 3: Input Motion Selection

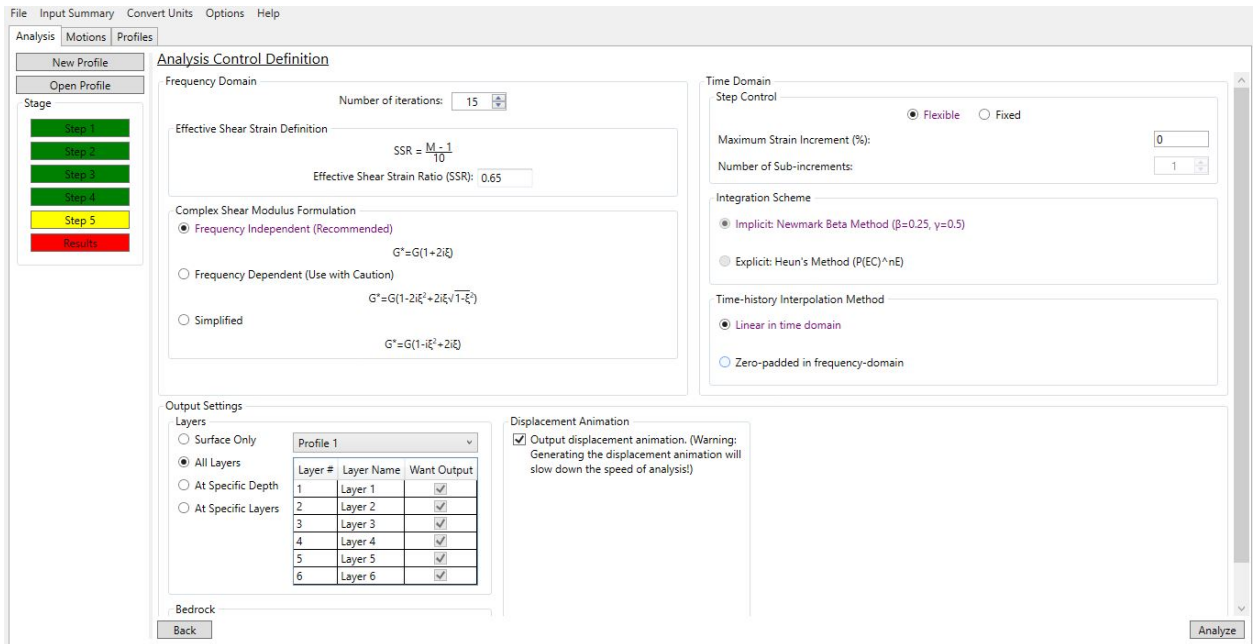**Figure A.12:** Step 4: Viscous/Small-strain Damping Definition
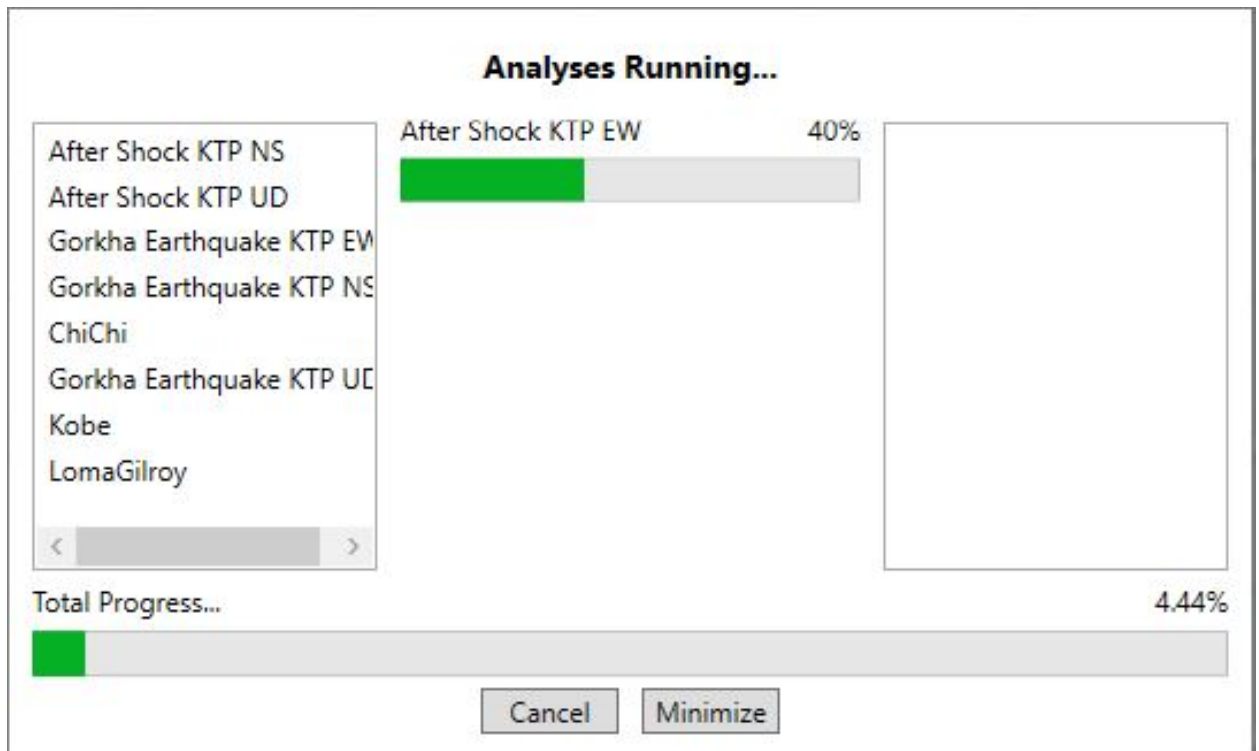
Figure A.13: Step 5: Analysis Control DEfinition

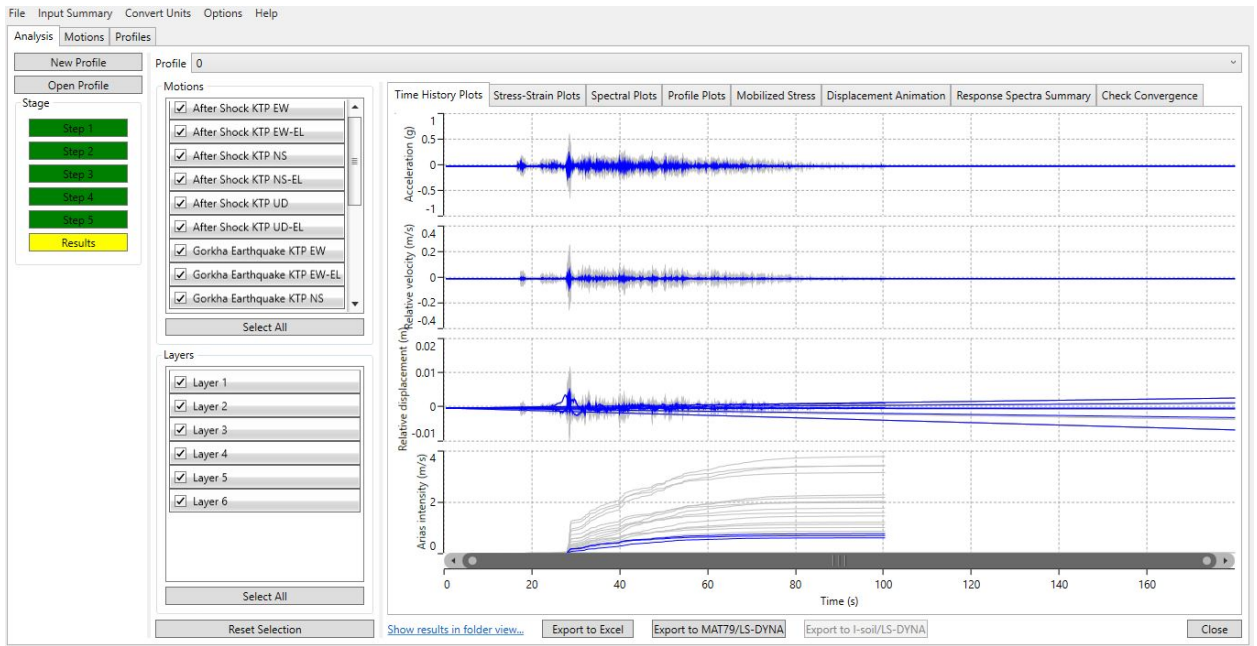

Figure A.14: Step 6: Analyses Running

Figure A.15: Step 7: Output Platform

APPENDIX D: LIST OF PUBLICATION

Conference paper

S.P. Adhikari, R.C. Tiwari and K. Pokhrel, "Comparative Study of Amplification Factors for Different Earthquake Scenarios in Kathmandu Valley," in *14th IOE Graduate Conference(2023)*, Lalitpur, Nepal